Mimicking the thigmotropic behaviour of climbing plants to design a tactile-based grasping device for the space environment

Final Report

Authors: R. Vidoni[1] , T. Mimmo[1], C. Pandolfi[2]
with the cooperation of S.Cesco[1] and F. Valentinuzzi[1]

Affiliation: [1]FAST-Faculty of Science and Technology, Free University of Bolzano, Bolzano (Italy), [2]ESA ACT- *Advanced Concepts Team*

Date: February, 2013

Contacts:

Renato Vidoni
Tel: +39 0471 017203
Fax: +39 0471 017009
e-mail: renato.vidoni@unibz.it

Leopold Summerer (Technical Officer)
Tel: +31(0)715656227
Fax: +31(0)715658018
e-mail: act@esa.int

Available on the ACT website
http://www.esa.int/act

Ariadna ID: 12-6402
Ariadna study type: Standard
Contract Number: 4000105988/12/NL/KML

Mimicking the thigmotropic behaviour of climbing plants to design a tactile-based grasping device for the space environment

ESA-ACT - UNIBZ

FAST - Faculty of Science and Technology
Free University of Bozen-Bolzano
Piazza Università 5, 39100 Bolzano - IT

Contents

Overview of the project

Development in 4 phases:

1. **Literature review and plant monitoring**
2. **Grasping behavior and elasto-mechanical models**
3. **Smart alloy biomimetic principles and tendril**
4. **Bio-inspired tendril...model, simulation and emulation**

1 Phase: Literature review and plant monitoring

Abstract. *The task of finding innovative concepts and solutions for understanding and mimicking the grasping and pulling behaviour and the flexibility of tendrils is tackled in this work. After a brief explanation of the physiological and biological behaviour of the climbing plants that develop tendrils, the three different thigmotropic phases are evaluated and discussed. Then, by means of an experimental set-up, two different climbing plants that develop tendrils are evaluated in order to better understand the grasping behaviour, the surface recognition, the signal transmission and the pulling up of the stem. Finally, results and directives for the work are outlined.*

Keywords: Tendrils, grasping, coiling, climbing

1.1 Introduction

This work aims at studying the particular rules and strategies behind the climbing plants that exploit tendrils from a bio-mimetic point of view. Such analysis will tackle these aspects in order to "read" the natural grasping behaviour also from an engineering point of view. Indeed, both a mechanical/robotic design phase and a motion planning and controller synthesis definition require a deep comprehension and evaluation of the plants principles. In this attempt the first phase of the project has been addressed.

1.2 Climbing plants and tendrils

Climbing plants have been usually classified according to the attachment mechanisms in five classes [15, 28]:

1. Twining plants (e.g., Dioscorea spp., Dioscoreaceae; Ipomoea spp., Convolvulaceae)
2. Leaf-climbers (e.g., Clematis spp ., Ranunculaceae; Bauhinia spp., Caesalpiniaceae)
3. Tendril-bearers (e.g., Vitis spp ., Vitaceae; Passiflora spp., Passifloraceae)
4. Root-climbers (referred here as "clinging-climbers") (e.g., Parthenocissus spp., Vitaceae; Hedera spp., Araliaceae)
5. Hook-climbers (e.g., Uncaria spp., Rubiaceae; Calamus spp., Arecaceae)

This work focuses on tendril-bearer plants.

Tendrils are long, slender, filiform, irritable organs, derived from stems, leaves, or flower peduncles [15] which may occur either as un-branched or multi-branched organs with a variable length ranging from 3.8 cm in Bignonia unguis (Bignoniaceae) to 20 cm in Passiflora spp, and 40 cm in Vitis vinifera (Vitaceae) [34].

The perception of thigmic stimuli is a widespread phenomenon among plants with decisive meaning for the ability to survive. Besides a general sensitivity for mechanical stimuli, many plants have evolved specialized organs with highly developed mechanisms to perceive and transduce the applied forces [19]. Mimosa pudica Linn. for example, responds to touch folding up its leaflets, and propagates the stimulus from one leaflet to the adjacent one and, if the stimulus is strong enough, it propagates even to adjacent leaves [61]. As far as touch induced movements might concern, tendrils are able to coil around a support and grasp it, enabling the plant to achieve vertical height without a proper supporting trunk.

Tendrils have shown to have three main movements [34]:

- circumnutation, an endogenous movement increasing the probability of contact with supports,
- contact coiling, in which the stimulated tendril coils around a support, and
- free-coiling, in which the tendril develops helical coils along its axis, not necessarily as a result of stimulation.

1.2.1 Circumnutation

Circumnutation is an oscillating growth pattern in rapidly elongating plant organs, such as roots, shoots, branches and flower stalks. It was well known to 19th-century plant scientists as nutation until the Darwins (father and son, [17]) introduced the term "circumnutation", used to this day. Circumnutational oscillations are manifestations of the radially asymmetric growth rate, typical of elongating plant organs [55], but Darwin's close observation of the behavior of climbing plants, led him to speculate that they were "searching" for some upright support. Then, he widened his investigation to a large variety of species in which, however, he found no exception to his generalization that circumnutations must be a universal kind of plant movement [17]. Indeed, today we know that the widespread occurrence of circumnutations is even greater than Darwin had ever suspected. It occurs in dicots and monocots [7] gymnosperms, fungi, bryophytes (Ceratodon purpureus, [44] and algae (Spirogyra, [42]).

Although circumnutatory movements appear to have no useful purpose in the majority of the cases, in climbing plants, they have a crucial function in seeking mechanical supports.

In fact, the circumnutational movement sweeps the tendril about in circular, pendulum-like, zigzag-shaped or elliptical paths increasing the possibility to contact with a support. Maximum tendril circumnutation usually coincides with the period of maximal irritability of the organ [59]. The axis of the rotation usually follows the path of the sun as observed by Darwin [16]. The rotational behavior seems though related to the age of the tendril. Whereas younger tendrils show a concentric circumnutation, i.e. moving continuously in the same direction at each point of inflection, older more mature tendrils seem to follow an eccentric path, i.e. moving in reverse direction at each alternate point of inflection [69].

The shape and amplitude of this rotating movement is highly plant-specific and might be induced by different stimuli [66] (Fig.1). For instance, shoots of Phaseolus

spp. follow predominantly a circular and elliptical path with a radius of approximately 10 cm which can be reduced if the plant is treated with a growth inhibitor or increased if treated with plant hormones as gibberellins [54]. Tendrils of Passiflora spp. on the other hand, circumnutate in a rosette-like path. Circumnutation movements range from minutes to several hours and might even vary within the same plant. Plant species and type of plant organs, environmental conditions as light, temperature or gravity as well as chemical, physical and biological stimuli can be considered as the main factors influencing the period of circumnutation. With a ultradian rhythm two types of oscillations might be observed: 1) short period nutations (SNP, 10-60 minutes long) and 2) long period nutations (LNP - 1-8 hours) with a clockwise (cw) and counterclockwise (ccw) direction, respectively. The direction might change very rapidly as a consequence of gravity or mechanical stress/stimulus as rubbing or touching the plant organ [38]. SPN decreases with increasing temperature while increases with plant age. To date, little is known about the influence of environmental factors as light affecting the circumnutation period. It has been observed that red light slows down the circumnutational movement of Arabidopsis thaliana. The same plant species showed less frequent and less regular circumnutations with a lower amplitude when irradiated with green light than with white light.

As outlined, circumnutation is a quite complex and very variable plant behaviour depending on different parameters. Up to now, three mechanisms have been proposed trying to describe the generation of circumnutation: the first ascribes the circumnutation to endogenous properties, the second describes circumnutation as a result of gravity, i.e. exogenous and the third and most likely mechanism assigns circumnutation to both exogenous and endogenous factors.

The mechanisms behind the circumnutation are, at today, not perfectly known and, as underlined in [66], both a deeper study on the molecular mechanism and a better and wider description of the circumnutation parameters should be done.

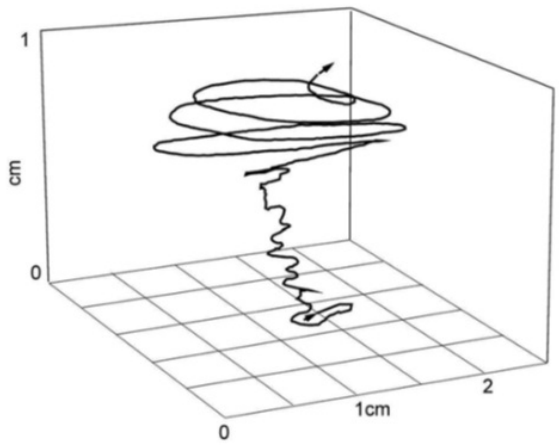

Figure 1: Example of circumnutations of Helianthus annuus stem tip during one day in the diurnal (lower part) and nocturnal periods (upper part). Picture taken from [66]

Figure 2: Branched tendrils coil (Lagenaria siceraria) around slender wire. Picture from: http://masteringhorticulture.blogspot.it/2010/07/tendril.html

1.2.2 Coiling

Contact coiling or simply coiling initiates as a response to a local mechanical stimulus of the tendrils which start curling around a support, see Fig.2, and tightening up [19], [71]. Since tendrils are often modified leaves or stems the contact coiling allows the plant to gain height or to turn the leaves maximizing sun exposure for the photosynthetic activity. In fact, some authors suggested that photosynthesis is a prerequisite for the winding movement as coiling could not be induced in the dark [19], [8]. If no suitable contact or support is found the tendril might even uncoil indicating that the process is reversible. The extent of the mechanical stimulus ranges from 1 to several mg as observed more than hundred years ago by Darwin [16] or even less than 1 mg (0.25 mg) as observed more recently by Simons [64]. Plants are also able to discriminate between stimuli; for instance, water droplets during a rain fall did not induce any coiling [33]. The tendril seems to perceive the stimulus/touch in the epidermal cells activating chemical signaling within the whole plant organ [50]. This response is very fast leading to a coiling within seconds. For instance, in Passiflora gracilis coiling occurred within 20-30 seconds [64]. Plant hormones as auxins or jasmonates have also been proposed to play a key role in the cell signaling and signal transduction of tendril coiling [70].

Many authors have demonstrated that the tendril coiling is associated to the production of gelatinous fibers, the so-called G fibers rich in polysaccharides. In tendrils these fibers form a cylinder-like structure of 5-6 cell layers between the vascular tissue and the epidermis [8]. The polysaccharidic matrix has a high hydration potential and favours the elasticity of the tendril movement. Though, with decreasing water content these fibers contract generating a contractile force and thus leading to tendril coiling.

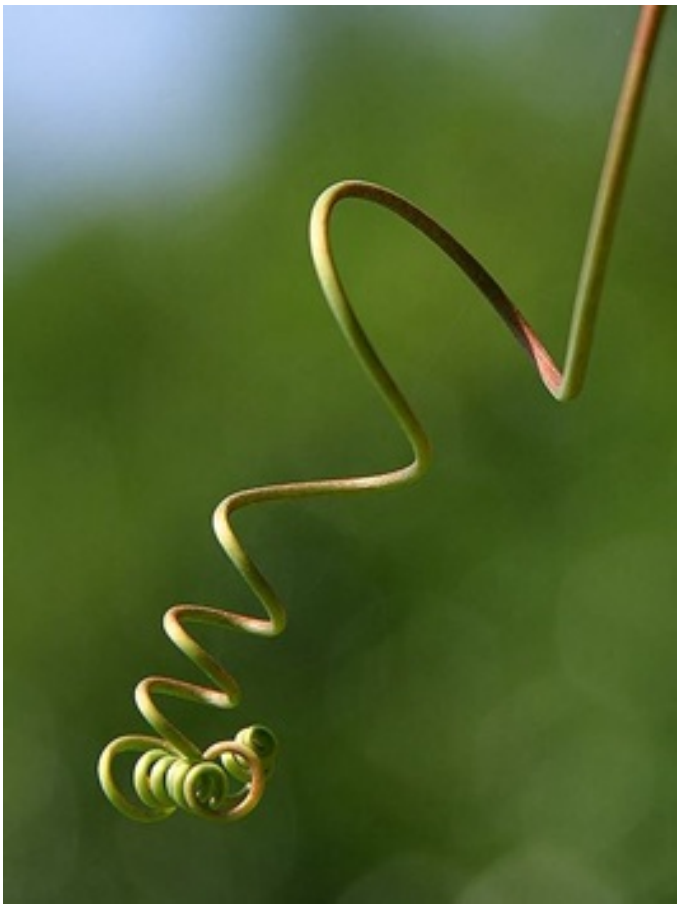

Figure 3: Free-Coiling, a curling tendril; source: http://en.wikipedia.org/wiki/Tendril

1.2.3 Free-coiling

Once the tendril has grasped around an object or support the plant organ undergoes a secondary coiling called free-coiling which brings the plant closer to the support. This movement creates an elastic spring-like connection able to resist to high winds and loads. Again, G fibers rich in acidic polysaccharides play a fundamental role during the rotational movement of the tendril. During the free-coiling the cell structure changes, G fibers dehydrate, lignify and get thus more rigid preventing an uncoiling. Usually, lignification is highest in the fibers closest to the touching surface [8]. This spiral structure has very often been compared to a telephone cord and might be described by an ideal helical spring. Free-coiling could happen, for example, in the beginning of senescence. Darwin [16] observed that there are the same numbers of spirals in both directions in order to compensate the twisting of the axis. The segment of spiral inversion which unifies the two helices is called tendril perversion often described starting from the Kirchhoff equation for thin elastic rods [22, 53]. If there is no grasp, the tendril curves and creates a sort of spiral as in Fig.3.

1.3 Materials and Methods

1.3.1 Plant Growth

Both pea (*Pisum sativum* L.) and passiflora (*Passiflora* spp) plants have been chosen to study the tendril development and growth. Pea seeds were germinated on moistened filter paper for 3-4 days in the dark at 20°C until each plant had one main root axis approximately 1.5 cm in length. The seedlings were placed in polypropylene pots containing organic soil and grown in a climatic chamber with a day/night temperature of approximately 26/19°C and a 10 hour photoperiod. Plants were irrigated every other day with a diluted Hoagland nutrient solution. Passiflora plants have been purchased and grown at the same conditions as the pea plants.

Round supports having a different diameter (4, 8, 14 mm) have been chosen to evaluate the coiling behavior. In addition, different shapes of the support have also been tested (Fig.4).

Figure 4: Shapes of the non-cylindrical supports used

For the round supports, at least six tendrils have been observed during the whole life-span (circumnutation, grasping and free-coiling). For the others, at least three tendrils each have been evaluated.

Regarding the response to mechanical stimulus, tendrils (n=3) have been hit in different points, Fig.5.

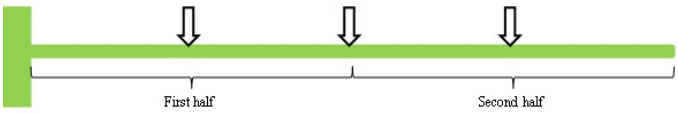

Figure 5: Influence on mechanical stimulus evaluation; arrows indicate where the tendrils are hit

1.3.2 Data acquisition

Tendril development has been recorded with HD web-cams (Trust eLight Full HD Web-cam, photo 8MPixel, 1920x1080 full HD video, Fig.6), acquiring images at fixed frame rates, e.g. every 30 or 60 seconds.

Acquired images have been consequently evaluated and post-processed by means of the Yawcam web-cam software [78], an open source software written in Java that allows to capture image snapshots from multiple web-cams, make time lapse movies and motion detection tasks.

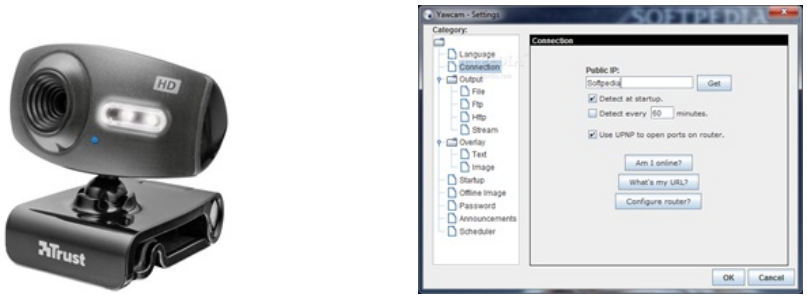

(a) (b)

Figure 6: HD web-cam (right), Yawcam software (left)

1.4 Results and Discussion

1.4.1 *Pisum Sativum* L.

Tendrils of legumes as *P. sativum* L. have been chosen to study the effects of mechanical stimulation on plant physiology, as extensively studied by Jaffe and Galston [29, 30, 31, 32, 34], Jaffe [35, 36] and Riehl and Jaffe [57]. Their tendrils respond to such a stimulus with a rapid coiling response to the dorsal side of the organ within minutes. In addition, plant species as legumes are useful because of their physiological features:

- long-distance signalling;
- fast plant growth;
- availability of mutants, particularly important for plant physiology studies [4].

Tendril coiling is a very useful plant trait used to screen specific stress markers (UV radiation and/or drought) by simple visualization. This characteristic can therefore be used for large scale screening experiments aimed at identifying components involved in stress signaling pathways.

1.4.2 Passiflora

Among the tendril plants, the Passifloraceae (Passiflora spp) as fast growing plant has been chosen together with the Pea plants. The passiflora is well known for its climbing behavior through axillary tendril development. Tendrils are present in the axial of a leaf closely associated with flowers.

Different experimental evaluations have been carried out in order to better understand the plant behavior and movement during the main phases of the tendril life.

The first phase, related to the thigmotropic behavior, is the circumnutation. Thanks to the experimental set-up previously described, the motion and active searching phase of the plants have been investigated in order to evaluate if circumnutation

takes place also during the night and if there is a preferred direction of nutation, i.e. clockwise (cw) or counterclockwise (ccw).

In order to answer the first question, tendril behaviours have been observed first of all recording the movement by switching the light off and on and, then, by observing the motion during the night (dark) period by means of the web-cam equipped with a led. Images and related videos show that circumnutation occurs also during the night and, moreover, that there is an intense/rich nocturnal activity (Fig.7). This results differ from the theories outlined by some authors [37, 19] which state that tendril circumnutation is related to photosynthetic activity.

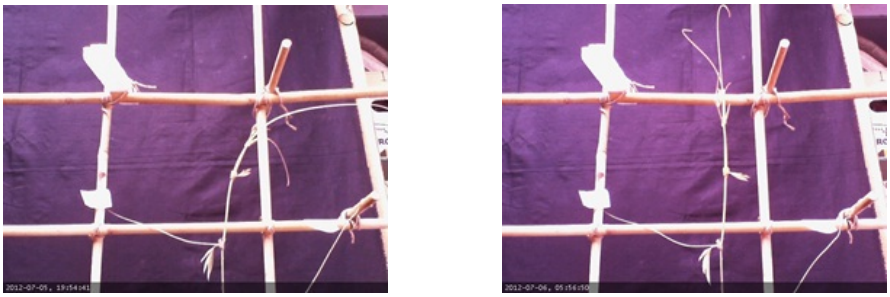

(a) (b)

Figure 7: Night motion: tendril condition at the switching off (sx) and at the switching on (dx)

In addition, experimental evidence showed that circumnutation in passiflora plants takes place indifferently both in cw and ccw directions (*see video Acircumnutation*) and in a preferred circular and elliptic shape.

Since the circumnutation motion occurs in the first phase of the tendril life, i.e. when the tendril grows and is touch sensitive, it can be useful to evaluate, also in a biomimetic perspective, if a contact/touch with a support or a surface stops the circumnutation phase. Experimental evidence on the passiflora plants shows that a mechanical stimuli cause a bending in the touching direction but are however not able to inhibit the circumnutation (*see video Acircumnutation*).

The second phase related to the thigmotropic behaviour is the contact coiling or simply coiling. When a support/surface is touched, the tendril bends in this direction trying to grasp it by coiling around the object. Hence, different questions arise:

- Does the tendril bend after a stroke? Does it recover the original shape or does it remain bent?
- Which is the irritable/sensitive area?
- How many coils are made?
- How is the signal transmitted? How can the tendril recognize edges and grasp flat surfaces?
- Does the tendril recognize either convex or concave surfaces?
- Does the tendril grow after the contact?

- Are there preferred shapes and dimensions of the support to be grasped?

Experimental evidence shows that:

- Carrington and Esnard [14] and Braam [6] previously evaluated and discussed the kinetics of the tendril after a stroke for watermelons and passiflora. Our experimental observations show that tendril recognizes the contact/stroke within seconds; however the bending towards the contact surface is quite variable in time (*see video Breflex*). It ranges from minutes to hours. For the passiflora, it seems that the recovery phase can be very slow or does not even occur.
- First evaluations show that tendrils are very sensitive from the central part to the apex (*see video Breflex*). Regarding the base, no experimental evidence of coiling after a stroke occurred. Tendrils have been hit at different points (1/4, 1/2, 3/4 of the tendril length) but no reaction could be observed in the lower part.
- The number of coils depends on the free part of the tendril, i.e. the part from the apex to the touching point, and on the shape of the support to be grasped. Indeed, if the support radius is too large, tendrils are not able to coil on the support and curl on themselves (Fig.8).
- Signal transmission is one of the most fascinating things to evaluate and discover in plants. In this case, when a tendril touches a support, the signal is most likely transmitted to the neighboring cells in order to induce bending in the touching direction but needs further physiological studies.
- By means of these observations, it is still unclear if the tendril is able to recognize the kind of shape. Indeed it seems that there is only a reflex behavior after the touch and not a "surface evaluation" phase.
- The tendril either grows or not after the contact, this is strongly dependent on the physiological status of the tendril.
- Tendrils grasp on different supports with different shapes and dimensions (Fig.9). Time-lapses and photos show that the tendril grasps on cylindrical and parallelepiped supports. This happens both for Passiflora and Pea plants. The coiling behavior depends on the dimension and geometry of the support that has to be coiled. Indeed, for small radii coiling occurs while, over a certain radius, only bending occurs.

Pea plants never grasp around cylinders with large radius (0.5 cm). However, they grasp l-shape supports (Fig.10).

The third phase related to the thigmotropic behaviour is the free-coiling.

During this phase the tendril changes its physiology and lignifies returning into its intrinsic spring-like shape. By considering this activity, the main questions that arise are:

1. Does the tendril always have a free-coiling phase or only if it has found a contact/support? When does the free-coiling phase start?
2. How many perversions are created and why?

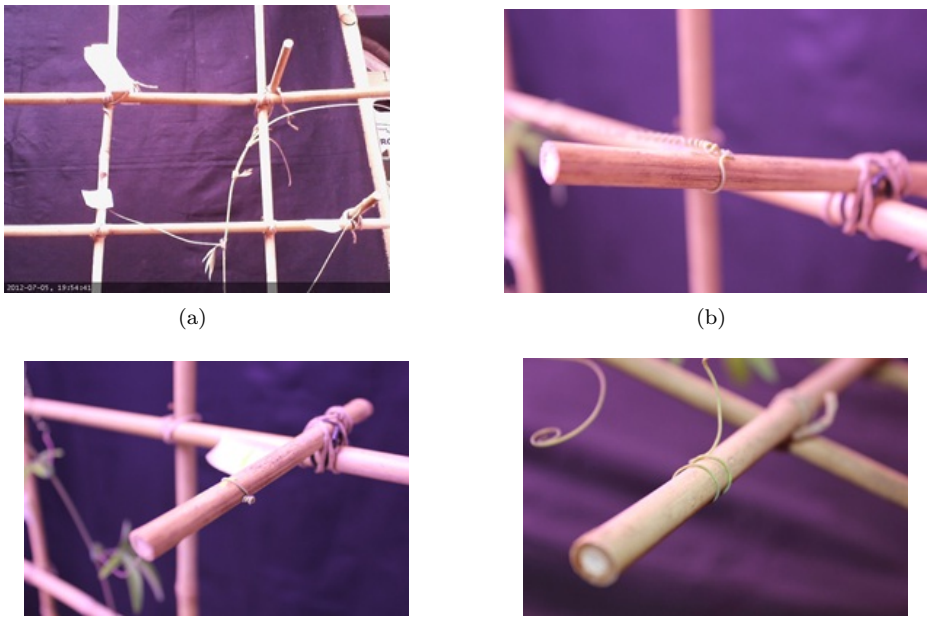

(a) (b) (c) (d)

Figure 8: Coiling: a) Pea; b,c,d) Passiflora

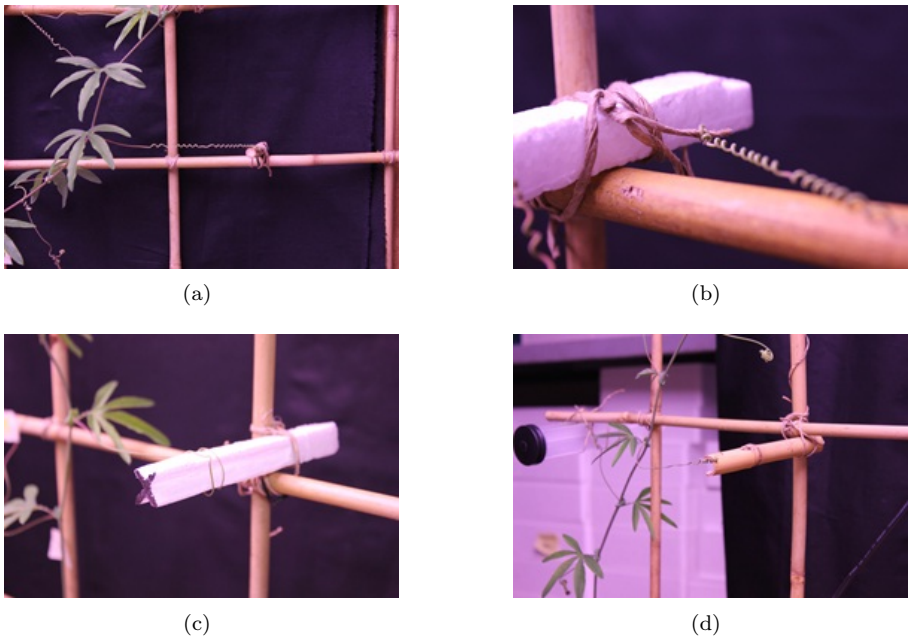

(a) (b) (c) (d)

Figure 9: Grasping on different shape supports - a) cylindrical, b)wire; c) cross; d) C-shape

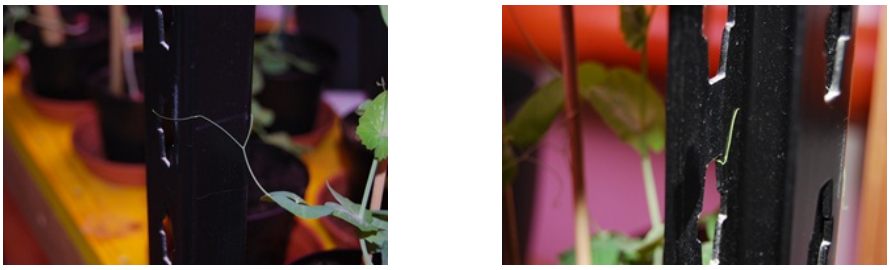

(a) (b)

Figure 10: Grasping of *P. Sativum* L. on a special shape support

3. If two different tendrils are grasped on different supports in different and opposite directions and the free-coiling phase starts, what happens? Is the final configuration in an energetic equilibrium or something else?

Experimental evidence, i.e. observations, photos and videos, shows that:

1. the free-coiling phase always occurs at the end of the active life of the tendril, i.e. after circumnutation and coiling. If grasping occurs, the stem will be brought towards the grasped support with a free-coiling phase. If no grasping occurs, there is a free-coiling of the tendril without perversion since one end of the tendril can twist.
2. The number of perversions is not constant. In our opinion it depends on different parameters such as the position of the extremes, the load (stem) to be moved and raised and the force that the free-coiling phase can create.
3. The free-coiling phase occurs for both the tendrils; depending on the grasping points, the tendril lengths and supports, an (energetic) equilibrium is found. This means that tendrils are not able to choose a preferred direction/strategy.

1.5 Conclusions

In this phase, climbing plants that create and use tendrils to find and grasp supports, and pull up its stem have been evaluated and investigated for biomimetic purposes. First of all, literature has been carefully evaluated; then, an experimental set-up has been defined and created to evaluate the different life phases of the tendrils and the grasping behavior. Finally, experimental tests have been performed to confirm some behaviors and show interesting and not yet well known activities. In particular the experimental results obtained with pea and passiflora plants have led to the following conclusions:

- the tendril activity occurs both in diurnal and nocturnal hours, i.e. with and without light, and is thus not related to photosynthetic activity;
- the touching-grasping phase seems to be driven only by a reflex behavior, i.e. without any possibility to select and/or refuse the touched support if not suitable for the plant climb;

- there is a dimensional limit on the supports that a tendril can grasp;
- the free-coiling phase occurs always and at the end of the tendril life;
- the free-coiling phase can be viewed as a passive grasping behavior that helps to straighten the grasp and pull up the plant.

In the next phase, a deeper investigation, in particular for points b), c) and e) is going to be carried out.

2 Phase: Grasping behavior and elasto-mechanical models

Abstract. *Following the results of the investigation of the growing and grasping mechanisms of tendril-based climbing, this phase focuses its attention on the deeper investigation on some specific behaviors and the translation of these results into engineering models, rules and ideas.*

Keywords: Tendrils, grasping, kinetics, springs

2.1 Modeling and validating the tendril behavior

2.1.1 Coiling: critical radius

Goriely and Neukirch [21, 56] and Isnard et al. [27] evaluated and discussed the mechanisms of climbing and attachment in twining plants. Goriely and Neukirch [21, 56] modeled the filament as an uniform elastic rod with a circular cross section, inextensible, unshearable and with constant intrinsic curvature and twist. Then, they evaluated the possible contact with a cylindrical support. By exploiting the Frenet frame notation and the Kirchoff's theory on elastic rods, they developed and simulated a model to find the limit radius of the support to which the elastic filament can coil up.

In twining plants, the stem coils around vertical supports while growing and this has many similarities with the grasping phase of the tendril. Therefore, the same model and results can be exploited to evaluate if the tendril is able or not to grasp a support by coiling up on it.

In the cited work, two different behaviors can occur. If the available length for coiling is sufficient, depending on the ratio between the intrinsic curvature of the filament and of the circular cross section of the support, the filament is able either to coil the cylindrical support or not. In this second case, only a short part of the tendril is in continuous contact with the support and the remaining part creates a sort of hook, showing an anchor-like behavior. The critical limit value is between 3 and 3.5. This means that the model forecasts a coiling behavior if the radius of the support $R \leq 3 \div 3.5^{*} r$, i.e. the intrinsic radius or the tendril coil.

To verify if this behavior could be observed also on tendrils, the following experimental set-up has been used:

- Cylindrical supports with different radii have been placed close to passiflora plants, and the grasping behavior of their tendrils have been recorded with a time-lapse camera.

Thus, let r = 1÷1.25 [mm] be the radius of a passiflora tendril and R = the radius of the support, by defining $\rho_0 = R/r$, the critical ratio ρ_c becomes 3÷3.5.

Thus, if $\rho_c = 3.3$ and $r = 1.25$ [mm] are chosen, the $R_{lim} = \rho_0{}^{*} r = 3.3 * 1.23$ [mm] = 4.125 [mm].

Again, if $r = 1.5$ [mm], $R_{lim} = \rho_0 * r = 3.3 * 1.5$ [mm] $= 4.955$ [mm].

In order to validate such a condition, the first support has been chosen with a 4 [mm] diameter, $r = 2$ [mm], hence inner the cited critical value. As can be appreciated in Fig. 11, the tendril easily coils on this kind of support.

The second evaluated support has a diameter of 10 [mm], hence a radius $r = 5$ [mm], just greater or at least equal to the computed critical value. Again the experimental observations and findings confirm the limit: Fig.12 shows that the tendril is not able to coil on this kind of support but creates a sort of hook.

Fig.11 and Fig.12 highlight a particular and not yet described behavior. Indeed, the last free part of the tendril, not able to coil the support, creates a particular and strong hook. This is due since the plants under study have a different behavior with respect to the twining plants. In particular, tendrils show a free-coiling behavior at the end of their life. This means that, in the evaluated case, the free part of the tendril that is in charge of creating a hook, twists and curls due to the free-coiling phase creating a better hook/anchor (i.e. creates a greater contact surface, Fig.13).

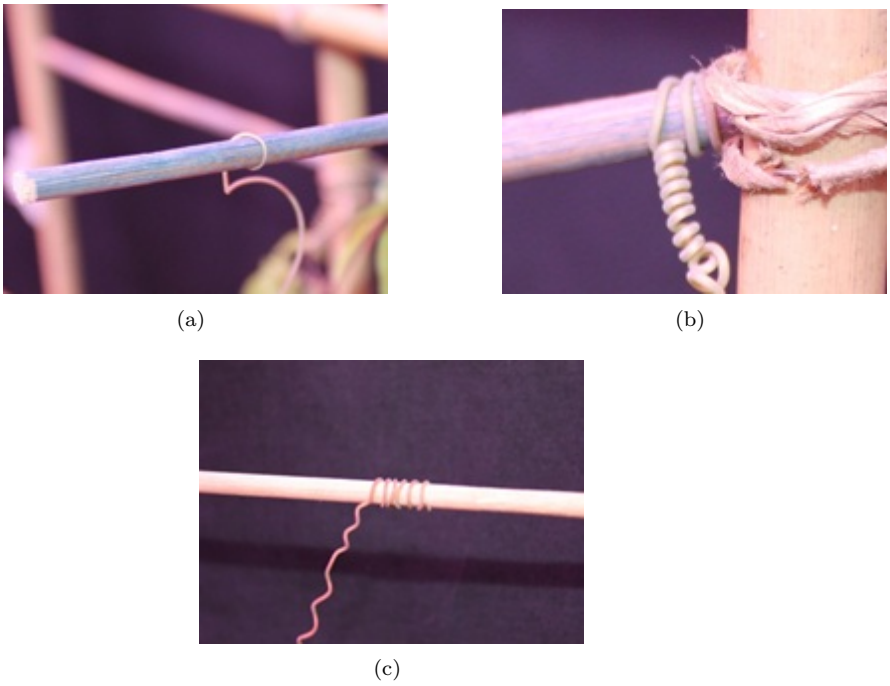

(a) (b)

(c)

Figure 11: Tendril coiling on a support with radius $r = 2$ [mm]

2.1.2 Coiling: touching point

By observing the tendril behavior during its life, it can be noticed how it shows a greater sensibility in the distal part. This is a reasonable and optimized behavior since the further the touching point, the greater the shortening of the tendril due to the free-coiling phase. Fig.s 14,15 show two tendrils in contact with a proper support: the first, in the upper part of the figure (Fig.14), touches the support at about its half; the second, in the lower part of the figure (Fig.15), touches only with

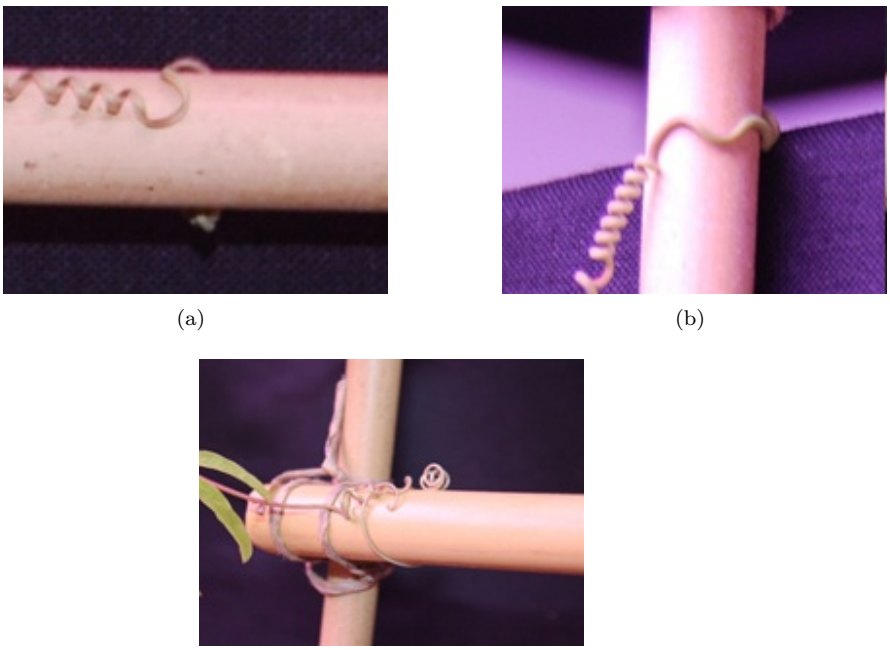

(a) (b)

(c)

Figure 12: Tendril grasping on a support with radius $r = 5$ [mm]

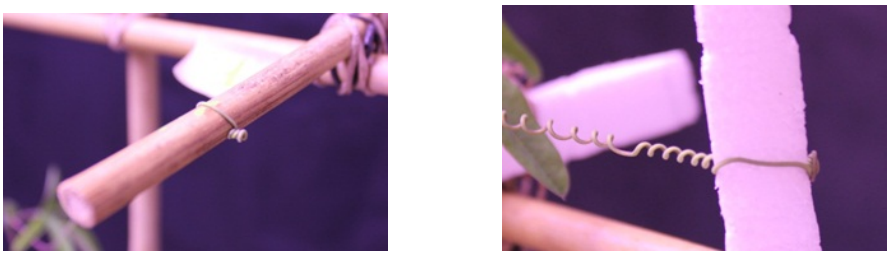

(a) (b)

Figure 13: Tendril grasping and hook/anchor creation due to the free-coiling phase

its final part. In both cases, the tendrils first bend in the direction of the contact and then grasp the support and coil. The number of coils is directly related to the free tendril length after the touching point.

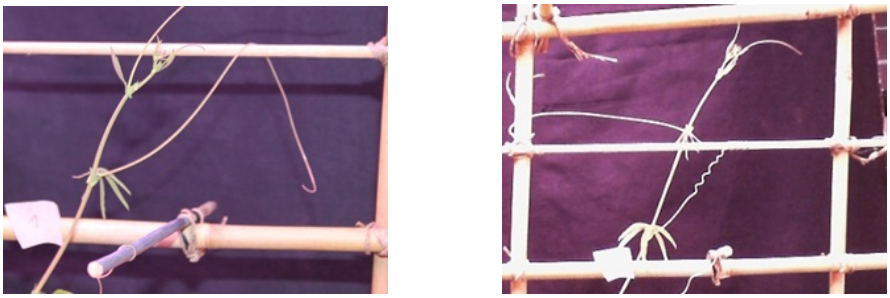

(a) (b)

Figure 14: Tendril coiling

(a) (b)

Figure 15: Tendril coiling

2.1.3 Coiling: non cylindrical supports

Several supports of different non cylindrical shapes have been evaluated to understand the behavior of the tendril. Indeed, the coiling behavior is perfectly suitable to rounded, elliptical, curved convex shapes. However, in nature surfaces have different shapes, not only convex or curved.

To evaluate the tendril grasping behavior in case of particular shapes, e.g. concave, cross, different supports have been created. In particular, the following supports have been evaluated:

- CROSS-LIKE SUPPORTS

Fig.16 shows a tendril in contact with a cross-shaped support (diagonal of 20 [mm]): it touches the support with its apex; the tendril is not able to make a coil but it creates a hook that strengthens by the free-coiling phase.

In Fig.17, the tendril has been placed on the cross support at about its half and wrapped around it; Two coils are created. Thanks to the free-coiling phase, the tendril is able to adapt to the shape of the support, thus strengthening the grasp.

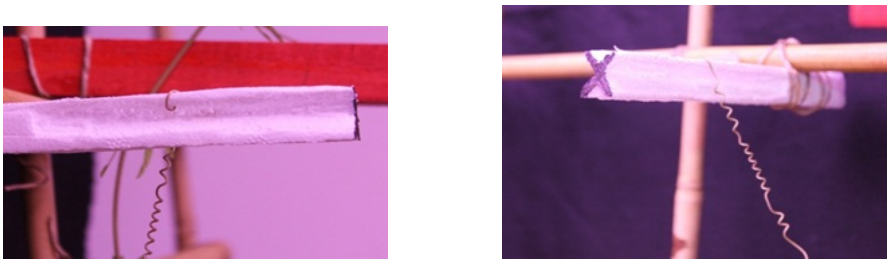

(a) (b)

Figure 16: Tendril grasping on cross-shaped supports: natural grasping

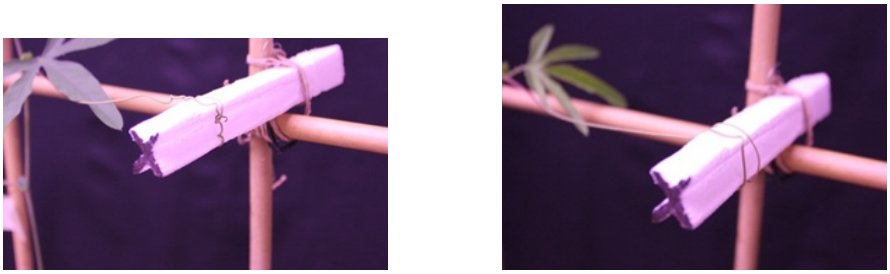

(a) (b)

Figure 17: Tendril grasping on cross-shaped supports: induced grasping

- SQUARE-SHAPED SUPPORTS

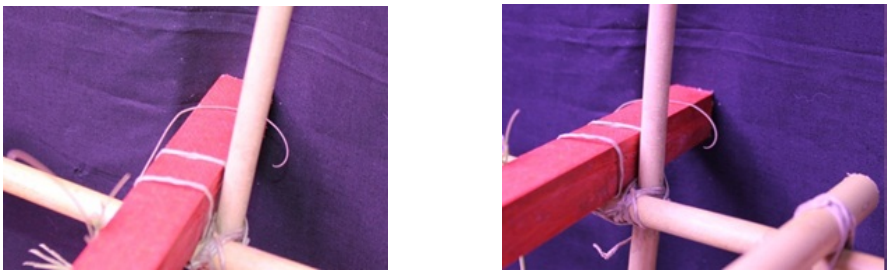

(a) (b)

Figure 18: Tendril grasping on a 20 x 20 [mm] square-shaped support

Fig. 18 and19 show a tendril that has been put in contact with square supports of two different sizes: 20 x 20 [mm] and 10 x 10 [mm]. In the first case, (Fig.18), the tendril is not able to grasp and coil. On the contrary, with the support of 10 x 10 [mm], (Fig.19), the tendril grasps without doing a coil since the free length is not sufficient. However, in this situation, a hook is created and then, thanks to the free-coiling phase, the "strengthening-spring" is created.

Similar considerations can be made considering the following shapes (Fig.20, 21):

- TRIANGULAR-SHAPED SUPPORTS

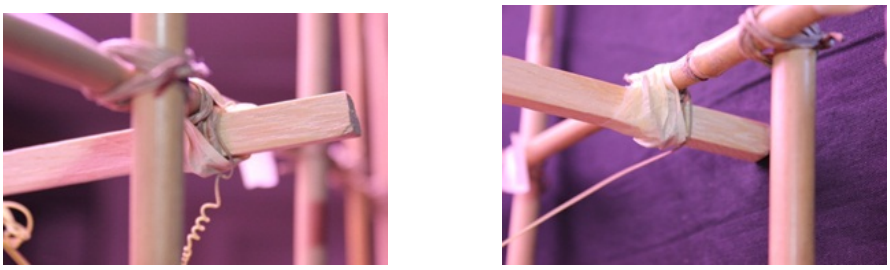

(a) (b)

Figure 19: Tendril grasping on a 10 x 10 [mm] square-shaped support

(a) (b)

Figure 20: Tendril grasping on a triangular-shaped support

- C-SHAPED SUPPORTS

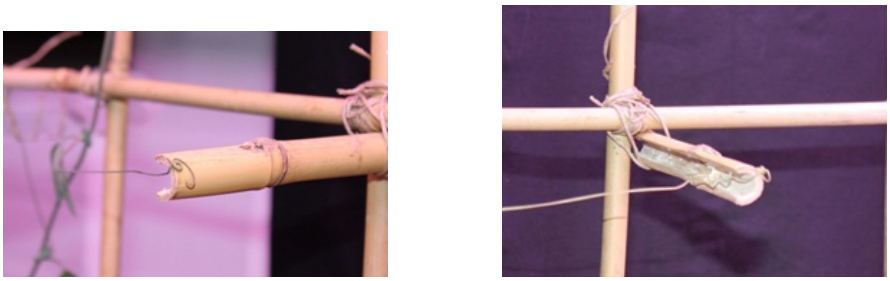

(a) (b)

Figure 21: Tendril grasping on a C-shaped support

When supports of other shapes like a triangle (15 [mm] side) or a “c” (diameter 15 [mm]) are evaluated, the tendril is not able to create coils. The grasping phase results in a hook.

2.2 Spring Behavior

This section discusses the spring/elastic characteristics of the tendril.

Looking at the spring-related classical mechanical theory, some important considerations can be done by considering both ideal and helical springs. The first one follows the Hooke's Law:

$$F = K * x$$

where F is the applied force, x the displacement and K the elastic constant that is related to the geometrical and physical properties of the elastic element.

In order to clarify the helical spring behavior, the coil radius $R=D/2$, the number of coils N, the wire diameter d, the applied force F and the shear modulus G have to be defined (see Fig. 21, [10]).

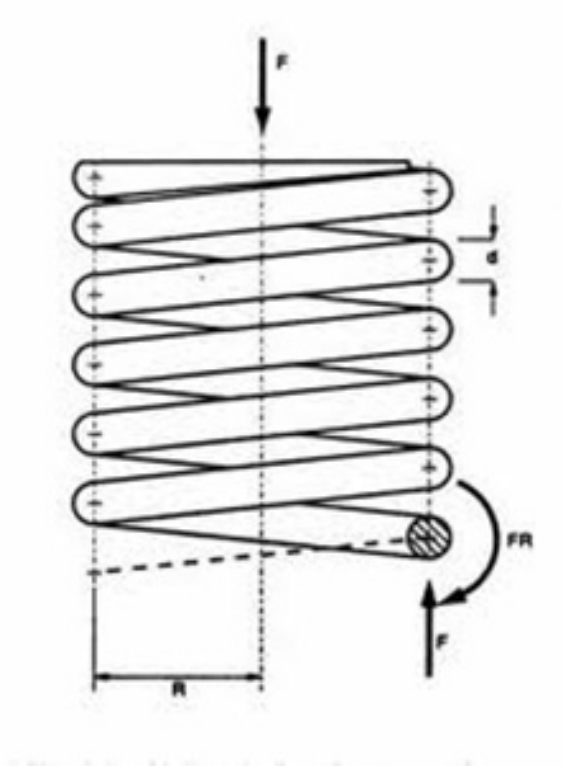

Figure 22: Helical spring

The elastic constant can then be computed as:

$$K = \frac{G * d^4}{8 * D^3 * N}$$

As can be easily appreciated, increasing the number of coils N allows to decrease the helix stiffness K; thus, generally speaking, less coils allow a greater resistance.

Moreover, if two springs are put in series, the equivalent stiffness K results:

$$K = \frac{1}{\frac{1}{k_1} + \frac{1}{k_2}}$$

in case of two springs with the same stiffness k_1, the resulting K is $k_1/2$.

Generally speaking this means that, assuming the perversion effect negligible, the tendril with perversion has to show a stiffness about half of the stiffness of a single helix (note: values have to be normalized with respect to the relaxed length or wire length). Recently, Gerbode et al. [20], investigated the elasticity of the tendrils by evaluating both bending and twisting stiffness and the age of the tendril, and found a direct relation between these two values and the tendril coiling, perversion creation and over-winding behavior.

Looking at the experimental graph in Fig. 23, some considerations can be made, at least when the elastic Hooke term dominates. By supposing the perversion stiffness (much more) greater than the helical one, i.e. rigid, it is possible to say that, if two tendrils of the same relaxed length, one without and one with perversion, are considered, the total arc length S is in the first case about π*D*N; in the second case the number of coils is less than N since perversion occurs. As a consequence, if the relative displacement is scaled with respect to the total arc length, it is possible to manipulate the helical spring formula as follows:

$$K = \frac{G * d^4}{8 * D^3 * N} = \frac{G * d^4 * \pi}{8 * D^2} * \frac{1}{\pi * D * N} = K^+ * \frac{1}{S}$$

$$K\Delta L = \frac{K^+}{S}\Delta L = K^+ * \Delta L^*$$

This means that, for instance, if the same axial relaxed length L_0 is considered, the tendril with perversion will have a S smaller than the one computed for the non-perverted one being different the N number of coils. Thus, at equal displacements $L - L_0$ correspond a greater ΔL^* for the tendril with perversion. From another point of view, it means that in order to have the same force F, the tendril-perverted ΔL has to be greater with respect to the helical one. This can also be used to evaluate the difference between dotted and continuous curves in Fig. 23, [20].

From another point of view, the stiffness K is inversely proportional to the coil diameter D in a cubic way, showing that the lower the diameter, the greater the stiffness.

Thus, it is better to minimize the coil diameter and this explains why the free-coiling phase creates helices of small diameters to pull up the stem of the plant.

As an example, we evaluated two different diameters and their effect on the elastic constant.

If, for instance, a tendril with of total length of $L = 63$ [mm] is considered and $D_1 = 2$ [mm] and $D_2 = 3$ [mm] are chosen as the coil diameters, the number of spires and the K are:

$$N_1 = L/(\pi * D_1) = 10 coils \Rightarrow K = cost/(D_1^3 * N_1) = cost * 1/80 = cost * 0.0125$$

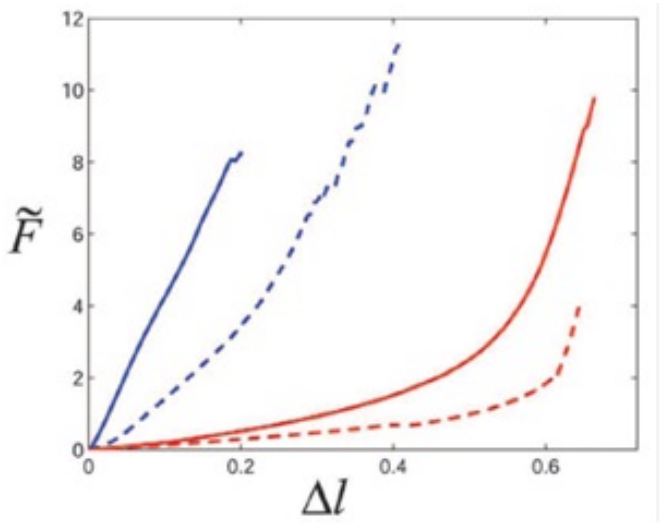

Figure 23: Difference between old and young tendrils (blue and red), without and with perversion (continuous and dotted), picture taken and modified from [20]

$$N_2 = L/(\pi * D_2) = 6.7 coils \Rightarrow K = cost/(D_2^3 * N_2) = cost * 1/181 = cost * 0.0055$$

Other important considerations can be made considering the particular dynamic conditions under which the tendrils have to work, i.e. no torsion, the models and results found in literature.

McMillen and Goriely [53] studied the perversion by modeling the tendrils starting from thin elastic rods described by the static Kirchhoff equations. This approach has been also followed by several authors [22, 77, 52, 3].

Regarding the spring characteristics, they approached the problem by evaluating how and how much a spring made by a perversion differs from the Hooke's law.

Following former results [53], for a spring made of perversion the following:

$$T = \frac{K^3\Gamma}{2\pi}\frac{d}{(1 - d^2\frac{K^2(1-\Gamma)}{4\pi^2})^2}$$

where T is the (scaled) tension, K the intrinsic (scaled) curvature in the axial direction, Γ is the ratio of torsional stiffness to the bending stiffness in the axial direction and d the displacement between two similar points in the helix.

In un-scaled terms, it holds:

$$T = h\frac{d}{(1 - d^2(1-\Gamma))^2}$$

with

$$h = K^2\Gamma EI_1 = 4\pi^2\Gamma EI_1$$

where I_1 is a term that depends on K, Γ and k, the constant curvature. If d is small, the deviation with respect to the Hooke's law is very small. If a spring made of helices is considered, it can be found that:

$$T = EI_1(\frac{K\tau}{(1-d^2)^{1/2}} - \frac{\tau^2}{d}$$

where τ is the torsion. Since d varies from d_0 to 1, T varies from 0 to ∞.

In the rest state, d=d_0 and, by calling $d^* = d$ - d_0 , it holds:

$$T = hd^* + O(d^{*2})$$

with h as follows:

$$h = EI_1 4\pi^2(1 + \Gamma EI_1 4pi^2 \frac{\tau_0^2}{K^2}$$

Again, if the relative displacement is small, the tension follows the Hooke's law and the "constant" is greater than the previous found for the perversion. Hence, a spring made of helices is stiffer than a perversion spring.

Looking at a real case, tendrils with perversion show the perverted area/part with a non-zero axial length; indeed, the perverted axial length is at least half of the total possible length. This means that in a relaxed state and for relative small displacements, if two equal helices of stiffness K are connected by means of a perversion, the perverted part (possibly) has a greater starting stiffness with respect to the other parts. Hence, the spring series equivalent stiffness results about $K/2$.

By implementing the formulas, clamped helices or perversion springs can be simulated. Fig. 24 shows different behaviors with d_0 set to 3.7 [mm] for the helices. Parameters have been chosen to mimic the experimental behavior. Again, the difference between a single helix and a series of two helices is similar to the experimental results.

Fig. 24 does not considered the perversion elastic effect. The generated tension increases fast (in a hyperbolic way) at relative large displacements. This behavior can allow an important conclusion: in the first phase of the free-coiling, i.e. when the fibers dehydrate to return to the original helical spring shape, the tendril seems to be capable of creating the maximum force. After that, thanks to this recalling force, it shortens the longitudinal length until an equilibrium between the load and the force exerted is found/reached. This suggests that the method of creating the free-coiling phase could be optimized in order to exploit the maximum possible force in the first phase of the pulling.

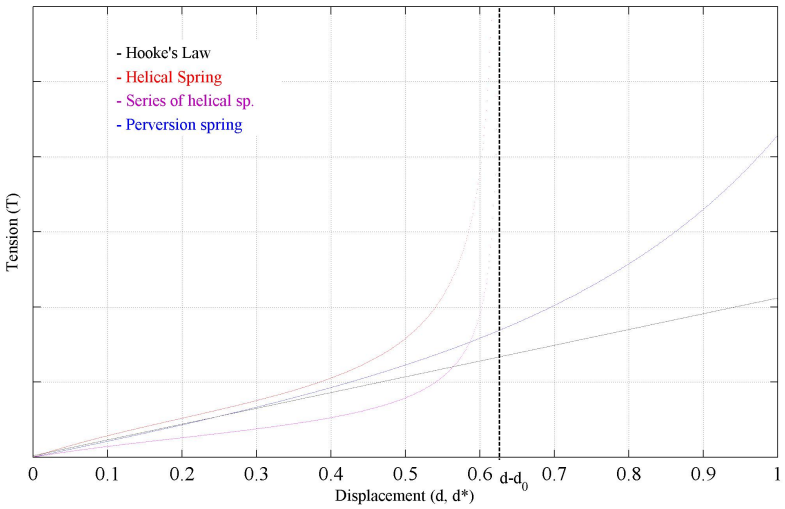

Figure 24: Simulation of the spring behavior

2.2.1 Perversion

The perversion, as describer for the first time by Darwin [16], allows to compensate the twisting of the axis since there it connects the same numbers of spirals in both directions.

The subtle physical mechanisms responsible for self-winding behavior is a result of the intrinsic curvature due to the non-uniform deformation of tendrils filaments. Indeed, due to the free-coiling phase at the beginning of the senescence, some fibers contract and change their elasticity, allowing in such a manner to recreate the intrinsic helical shape. The result, in case of constrained ending points, is a series of helices connected by means of perversions. No torsion is allowed since the ends of the tendril filament are constrained and, hence, the perversion phenomena results in a smart and necessary solution for allowing the free-coiling.

During and after the free-coiling phase, the real tendril can be considered as made of a series of helices and perversion springs. Looking at the formula of the perversion spring, a term related to the ratio between torsional and bending stiffness can be found.

Depending on its value, different behaviors can be underlined. if $\Gamma = 1$, the Hooke's law holds.

If $0 < \Gamma < 1$ or $0 <$ 1-$\Gamma < 1$, since D is < 1, the denominator decreases from 1 to a minimum and it is always different from 0.

if $\Gamma > 1$ or 1 - $\Gamma < 0$, the denominator shows a different behavior. It is always positive, greater than 1 and increases with the displacement. Thus, at a certain point/value, the related curve changes its behavior and the slope from positive to negative.

2.3 Tendril Measures

The tendrils elastic behavior and its dependence on the age, number of coils and perversions, have been experimentally evaluated measuring the elasticity of cut passiflora tendrils (Tab. 1 and Fig. 25).

Table 1: Evaluated tendrils; (*) length without coils; (**) number of coils per part

	Length [mm] (*)	Coil Diam. [mm]	coil N. (**)	perv	age	Tendril Diam. [mm]
Tendril1	63 (14)	3.5	14 (7)	1	old	1
Tendril2	64	2.5	14 (7)	1	old	0.6
Tendril3	98 (18)	2.5	18	4	old	0.6
Tendril4	53	1.5	18 (7-2)	3	medium	0.3
Tendril5	42 (20)	2	18 (9)	1	old	0.3
Tendril6	38 (18)	3	12	4	young	< 0.3
Tendril7	30 (23)	-	3	0	young	< 0.3
Tendril8	20 (15)	-	3	0	young	< 0.3

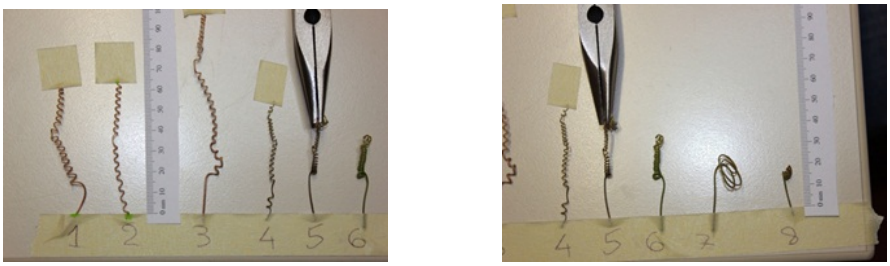

(a) (b)

Figure 25: Tendril samples

Fig.26 shows an experimental equipment to quantify and evaluate this. In particular, the system has been created to gradually change the load with which the tendril is pulled and, in the meantime, measure/quantify the relative displacement.

(a) (b)

Figure 26: Experimental test system

By measuring and taking snapshots of the equilibrium points, the displacement - force curve has been obtained. In this test, the displacement has been considered as: $(l - l_0)/l_t$ with l the measured length, l_0 the length at rest and l_t the approx. length of the uncoiled tendril.

- Tendril 6: 38 [mm] length (18 straight part length); 12 coils; 4 perversions; young tendril coil diameter 3 [mm].

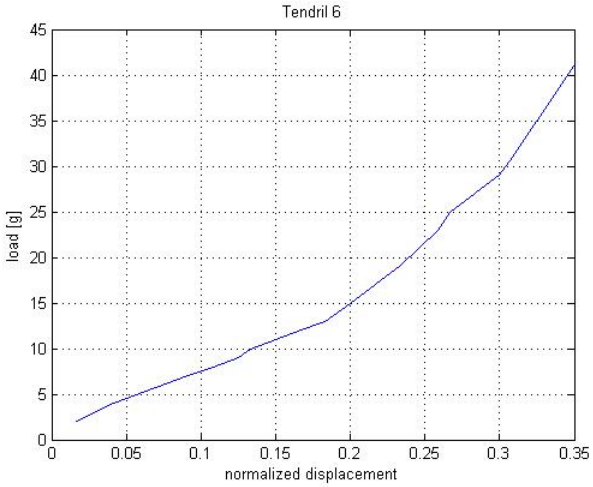

Figure 27: Tendril 6, displacement versus force

- Tendril 8: 20 [mm] length (15 [mm] straight part); 3 coils; no perversions; young tendril; no grasping. In this test, the displacement has been considered as: $(l - l_2)/l_2$ with l the measured length, l_2 the length when the load is 2 [g], i.e. the minimum for the experimental test-bench.

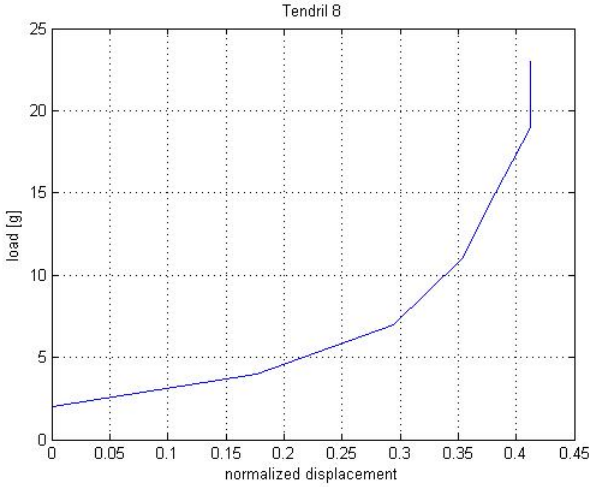

Figure 28: Tendril 8, displacement versus force

- Tendril 1: 61 [mm] length (14 straight part length); 14 coils; 1 perversion; old tendril coil diameter 3.5 [mm] To compare the two measures, displacement is here computed as $(l - l_0)$.

Fig.s 27,28,29 show the qualitative helix like behavior and the difference in stiffness between tendril with and without perversion. As reported in the cited papers, the

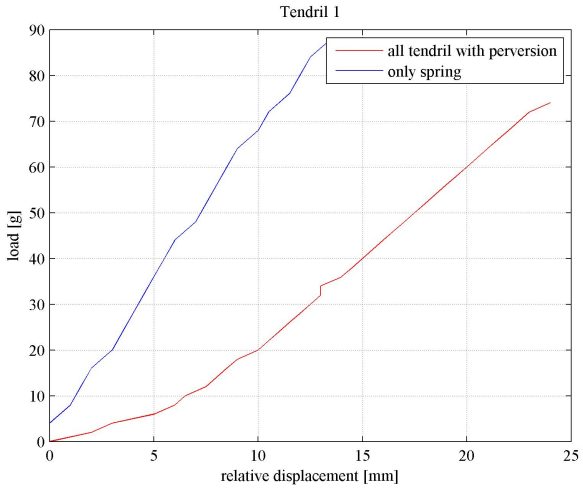

Figure 29: Tendril 1, displacement versus force

stiffness of an old tendril is greater than the one of a young tendril. This suggests that the forces, e.g. wind, that the tendril can manage are very high when it is grasped and dehydrated.

2.4 Conclusions

In this second phase, the tendril characteristics and behavior have been evaluated both to observe particular movements and to model and simulate mechanical and elastic properties, thus translating in technical language the experimental findings. Starting from the literature, we have demonstrated that there is a critical maximum radius in tendril like structures which does not permit coiling. One of the most fascinating things seen is that, even in that case, the system is able to grasp the support creating a hook. It is the free-coiling phase that strengthens and secures the grasping. The stiffness and properties of the system have been evaluated focusing on the free-coiling phase. Again, the system evolved to exert the maximum pulling force for high displacements, i.e. in the first phase of the free-coiling. In the next phase we will evaluate possible solutions for modeling and replicating these capabilities in a biomimetic way.

3 Phase: Smart alloy biomimetic principles and tendril

Abstract. *Following the results of the first two phases of the project, different materials and techniques are evaluated to mimic the basic rules behind the tendrils behaviour both to set-up future effective bio-mimetic mechanisms and to validate the experimental observations. In particular, the free-coiling phase has been focused both in terms of pulling and perversion, and in terms of grasp strengthening.*

Keywords: Tendrils, SMA, grasping, free-coiling, pulling

3.1 Smart materials

Biorobotics and bioengineering require new and/or special active materials for developing new robots and (micro)actuators and sensors. Thus, traditional materials such as alloys and metals are going to be replaced by polymers or special alloys. New intelligent materials are being used to sense the environment and respond accordingly. Shape-memory alloys (SMA), piezoelectric materials, electroactive polymers fall in this category of intelligent materials [76].

Significant applications of these materials can be found in biomimetics, i.e. keep inspiration from nature and design engineering devices [2]. Such materials are able to respond to external stimuli, e.g. electrical field, magnetic field, light, Ph, by changing shape or size, contracting, elongating, bending, etc. Hence, they can be the suitable materials for investigating, reproducing and mimicking the tendrils behavior. Electroactive Polymers (EAP) [43] are "smart materials" that, similarly to piezoelectric actuators, deform in the presence of an applied electric field . Unlike piezo-actuators, EAPs work and produce strain and deflections in a way similar to biological muscles [79].

SMAs are materials capable to return to a predetermined shape when heated. If cold, i.e. below their transition temperature, they show a low yield strength and can be easily deformed to a generic stable shape. If the material is heated above its transition temperature, a change in its crystal structure and a return to the memorized shape occur, also generating large forces if obstacles or resistance are encountered.

Shape memory alloys (SMA) exhibit large energy density and low driving voltage.

Generally speaking, two types of shape memory effects can be performed:

- one-way memory effect: it contracts to an original shape if heated; if no stress is applied, it remains in the hot shape when it cools down.
- two-way memory effect: if properly trained, it stretches back to an original shape at the low temperature. This means that two-way effect SMA show both contractive and tensile forces; contraction force is much greater than tensile force.

The temperature of the material drives the phase transition and the mechanical power generation. Joule effect is the most common way adopted but cooling can be performed also by conduction or convection. One-way effect SMA can be attractive in robotic applications, for instance when in a wire form.

Indeed, passive elastic forces or antagonistic SMA actuator pairs can be used to create actuators [24, 48, 45, 63, 65, 47]. One possible drawback in this applications is the slow response time and/or the hysteresis; the latter can be compensated by control algorithms while the former can be controlled by, for instance, a rapid heating or antagonistic actuation [74, 11]. With SMA, lightweight, silent and inexpensive actuators can be created [46].

In this work, among the possible solutions, the commercial available SMAs have been chosen as basic material. This has been done because the desired shape can be memorized in a relatively simple manner, they are sold both in wire and spring form and for cost reasons.

3.1.1 Nitinol

One of the most common SMAs is a nickel-titanium alloy: the Nitinol (NiTi).

Nitinol shows very good mechanical and electrical properties and a long fatigue life. For instance, a NiTi wire of 0.5 [mm] diameter can move 7 [kg]. NiTi is conductive and, thus, it can be heated by joule effect by passing an electric current through the wire to reach the transition temperature. This temperature is usually much more greater than the room temperature, thus allowing to exploit such materials as smart and small actuators and/or sensors.

Tab. 2 shows the main mechanical and physical properties of Nitinol.

Table 2: Nitinol properties

	Physical properties of Nitinol
Density	6.45 g/cm^3
Resistivity (Hi-temp state)	82μohm/cm
Resistivity (Lo-temp state)	76μohm/cm
Thermal capacity	10 W/mK
Heat capacity	322 J/kgK
Melting temperature	1240-1310 °C
	Mechanical Properties of Nitinol
Ultimate Tensile Strength	754-960 Mpa
Typical Elongation to Fracture	15.5 %
Typical Yield Strength (hi-temp)	560 MPa
Typical Yield Strength (lo-temp)	100 MPa
Approx. Elastic Modulus (hi-temp)	75 GPa
Approx. Elastic Modulus (lo-temp)	28 GPa
Approximate Poisson's Ratio	0.3

Fig. 30 shows the thermo-mechanical characteristics (both martensite - lo-temp - and austenite - hi-temp) of the SMA NiTi wires.

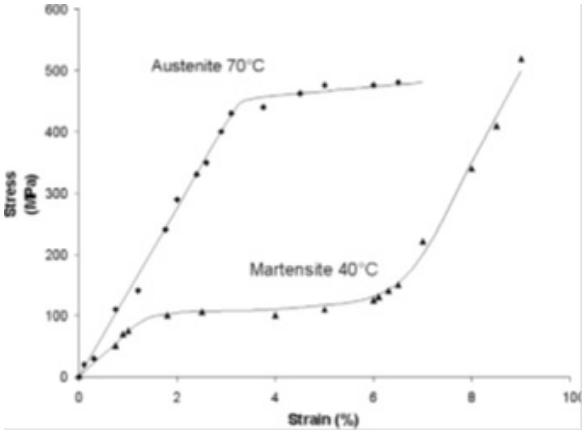

Figure 30: Stress-strain characteristics at different temperatures

NiTi wires have been used and their shape for the on-phase has been memorized by heating and maintaining the material in the desired shape for some minutes at a temperature between 500° and 800° with a controlled oven(Fig. 31).

(a) (b)

Figure 31: SMA NiTi: example of memorized shape: a) spring and b) spring with perversion

3.1.2 Flexinol^{TM}

Among the different patented SMAs, the Flexinol^{TM} [80], (Fig. 32), is of particular interest. It is manufactured by Dynalloy Inc. which is a manufacturer specialized in SMA actuators. Flexinol^{TM} is a nickel titanium alloy actuator manufactured as small wires able to contract like little muscles. In the "on" phase, when heated, their contraction is about 4-5%; when in the "off" phase they relay. Since they are utilized as actuators, they have to show high repeatability, i.e. they have to be a reliable and very repeatable material. Since they are Nichel Titanium alloys, they have the same physical and mechanical characteristics previously described for the Nitinol.

The exploited ability to flex or shorten is due to the change of the material internal structure; the effect is a silent and smooth movement, hence suitable for movements in small space with moderate speeds. Moreover, if properly driven a life of tens of millions of cycles is reasonable.

Often, in order to recover the original shape, an opposing constant force - bias force - is used. As the wire cools, the bias force elongates it. The wire strength, pulling and bias forces directly depend on the wire size.

Crucial is how the wire is made to operate. Normal bias springs allow 3-4% stroke, reverse bias forces allow to flex up to 7% and a coupled device can transform this stroke in a motion of over 100% the wires' length and provide, in the meantime, a bias force.

Figure 32: SMA Flexinol^{TM} wire

3.2 Mimicking and validating tendril principles

3.2.1 Grasping

One of the effects that we investigated for bio-mimetic purposes is a secondary effect of the free-coiling phase. Indeed, as shown in the previous phases, if the tendril has coiled and grasped a non-cylindrical support, e.g. with a rectangular cross section, the free-coiling phase allows a grasp strengthening and surface border adaptation. This happens when a hook is created for grasping the support.

Again, first of all we have investigated the phenomenon by means of a phone cord and then, by SMA.

The phone cord has been stretched and a grasping by anchoring has been induced by bringing the cord near to the support. By releasing the tension, the cord comes back to the original helical shapes. The final result is a cord grasped to the support with a better anchor, since a sort of "cap" is created (Fig.33).

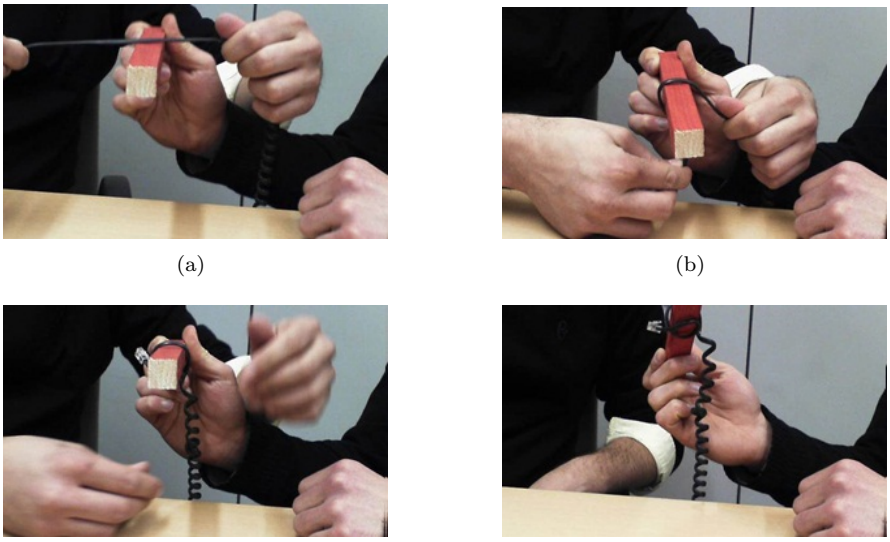

(a) (b)

(c) (d)

Figure 33: SMA Free-coiling enhancing grasping effect

As SMA, a NiTi wire of 1.25 [mm] diameter has been trained to recover a helical spring shape when heated. At room temperature it has been deformed and coiled around a rectangular cross section support; then, tension has been applied to heat the wire.

The effect, shown in Fig.34, confirms the idea: the phase transition and the change of shape induces the material to "take" the support form, hence increasing the contact surface and, as a consequence, friction force and strength.

3.2.2 Free-coiling and Perversion

As described in the previous phases, during the free-coiling phase, i.e. the phase in which the tendril recovers the original spring shape, if the extremities are constrained and torsion is not allowed, the perversion occurs.

Thus, if the tendril has grasped and the free-coiling phase starts, one extremity is anchored; the other cannot twist since it is fixed to the stem but can move if the created pulling force is greater than the stem/plant load.

This phenomenon can be appreciated and reproduced if a phone cord is firstly stretched, then constrained in its ending points and finally allowed to linearly shift only from one hand. To this end, an experimental test-bed has been set-up by means of a linear guide (Fig. 35).

Fig.s. 36 and 37 shows the sequence of perversion creation. In both the figures, it is possible to appreciate the perversion creation between two helical springs. In particular, when a long straight piece is kept as initial state, the generated coils on one side of the perversion are smaller in radius (last sub-figure in Fig. 37); this behavior/phenomenon often occurs also in the real plants. Concerning the pulling force, it is greater at the beginning and decreases with the shortening of the distance

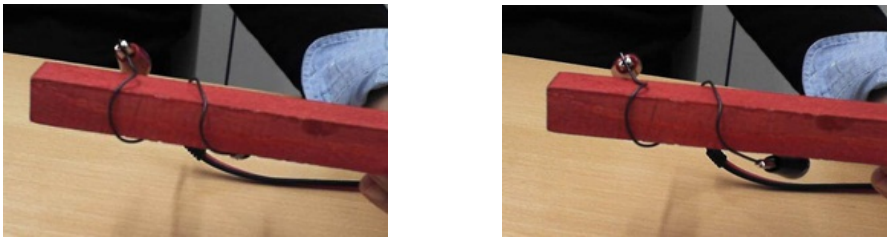

(a) (b)

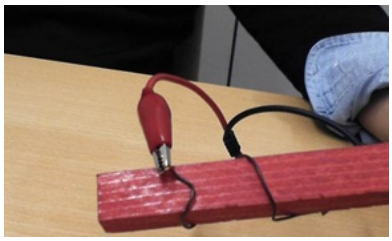

(c)

Figure 34: SMA Free-coiling enhancing grasping effect: a) starting point; b,c) SMA free-coiling effect

Figure 35: Test-bed for free-coiling emulation and evaluation

between the constrained end-points, thus with the relative displacement with respect to the rest configuration. Indeed, the force is able to move the linear guide, i.e. is greater than the static friction, only from a certain relative displacement.

This behavior, to our knowledge, has never been highlighted and investigated; its evaluation, modeling and deeper investigation can be surely object of future work.

By exploiting the SMA materials, in particular a trained NiTi wire, the perversion can be reproduced. First of all, a helical spring shape has been memorized and, then, the material has been stretched to an almost linear shape. After that, it has been fixed in order to not to twist, i.e. no torsion was allowed, and it has been heated. The perversion effect can be reproduced by means of SMA materials even if it is not repeatable for a large number of cycles due to the material performance degradation.

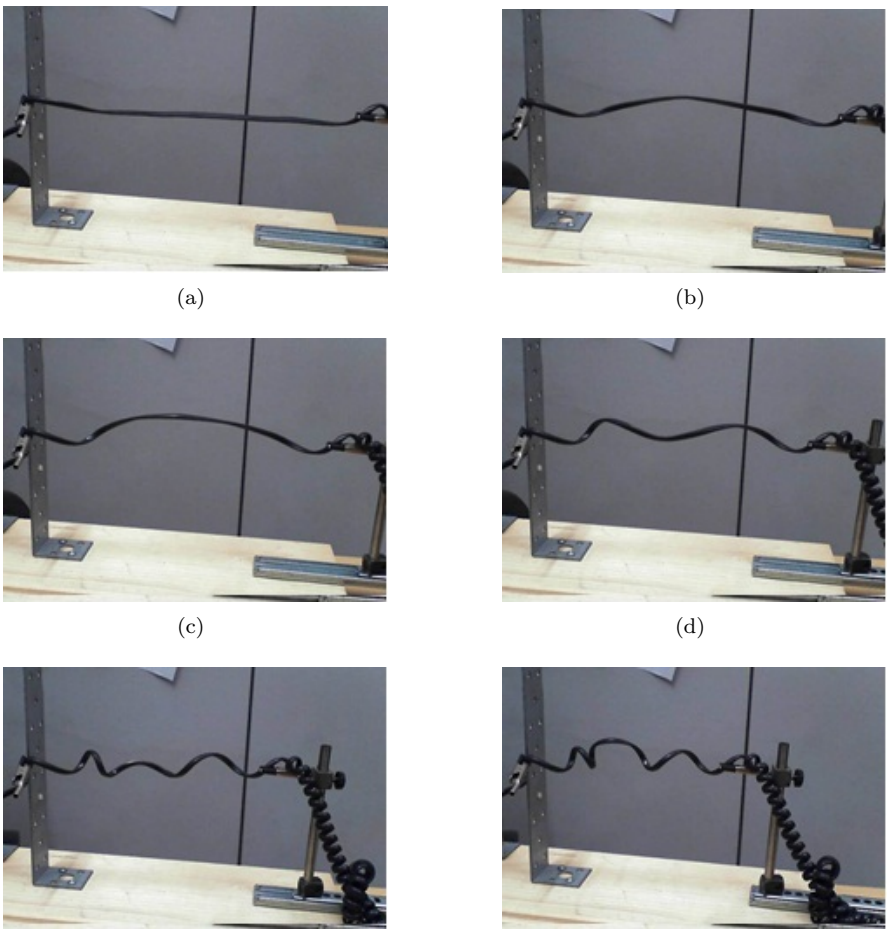

(a) (b) (c) (d) (e) (f)

Figure 36: SMA Free-coiling and perversion with a phone cord 1

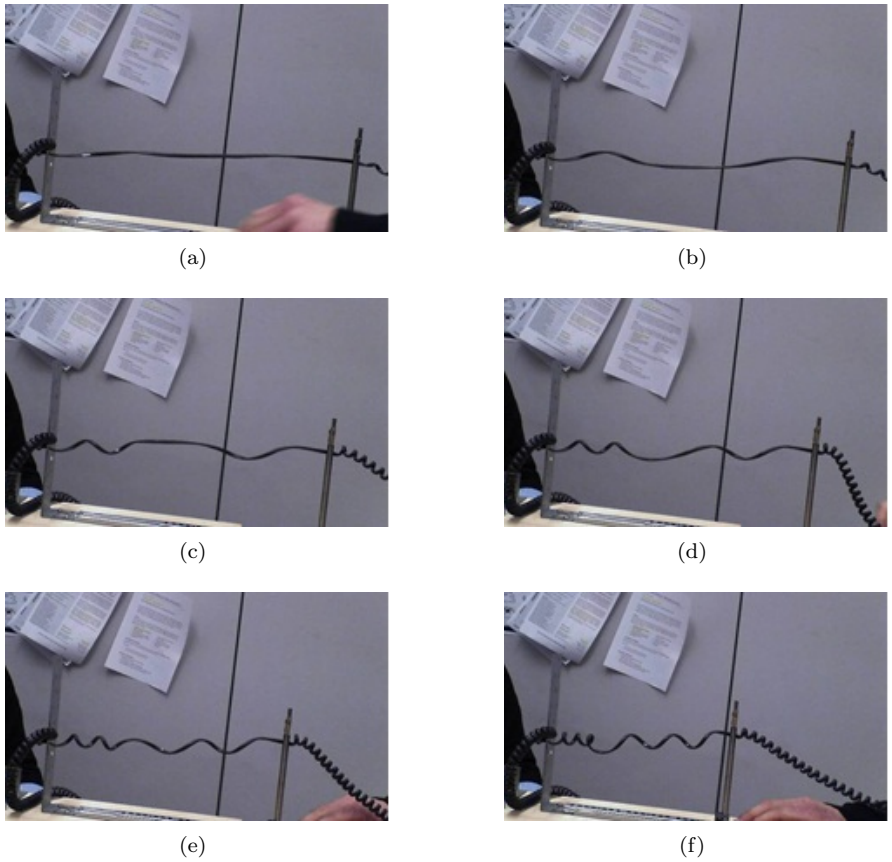

(a) (b) (c) (d) (e) (f)

Figure 37: SMA Free-coiling and perversion with a phone cord 2

Moreover, the effect can be better reproduced if the memorized shape is a series of two helical springs with opposite rotation direction connected by a perversion. Indeed, when in the off phase, the material can be stretched and made similar to a linear wire; its end-points can be constrained and cooled by applying a proper voltage/current. Since the final memorized shape does not require the torsion of the extremities, the SMA recovers well its original shape acting as a linear actuator. Clearly the same behavior could be reproduced by only a series of helical springs with opposite rotation direction. In Fig. 38 and 39, the phenomenon is shown.

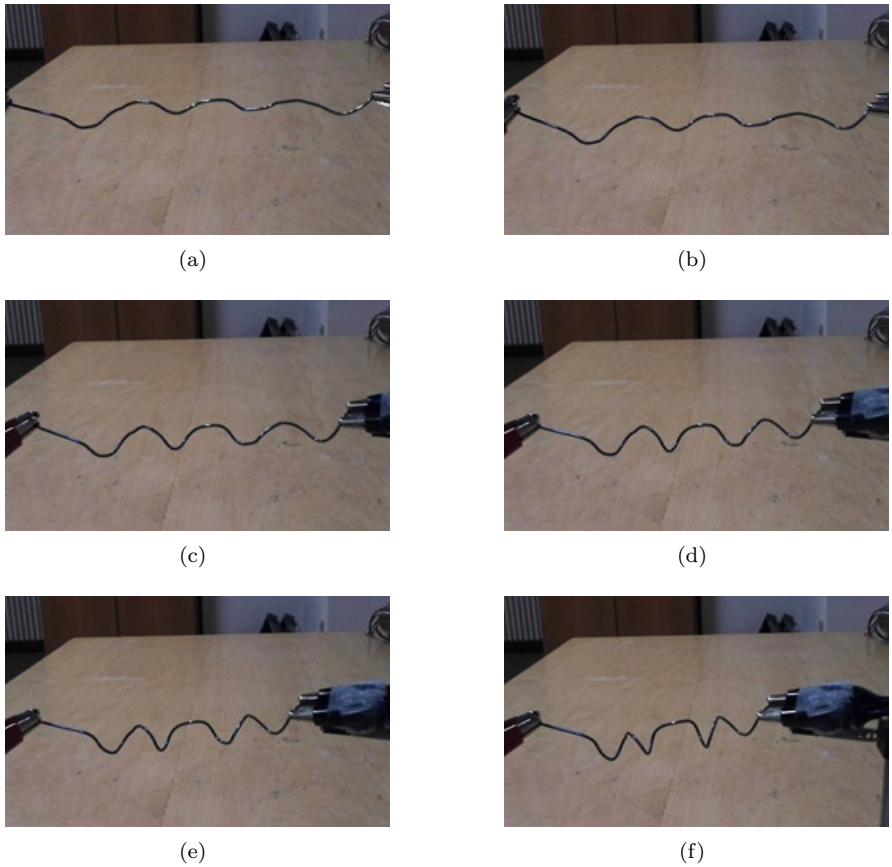

Figure 38: Free-coiling and perversion by means of SMA

3.3 Grasping behavior

As described in previous sections, tendrils life can be subdivided in three main phases: circumnutation, grasping by coiling or hook creation and free-coiling. If the grasping phase is focused to be reproduced by smart materials, the main limit is related to the reflex behavior; indeed, the tendril bends in the direction from which the contact is recognized. This means that, to replicate the grasping behavior, the SMA material could work well only if the touched support is able to induce a localized phase transition and, hence, a bending phenomenon in the material; this means that, for instance, the support should be hot enough or the tendril should be equipped with touch sensors and, thus, made not only by SMAs.

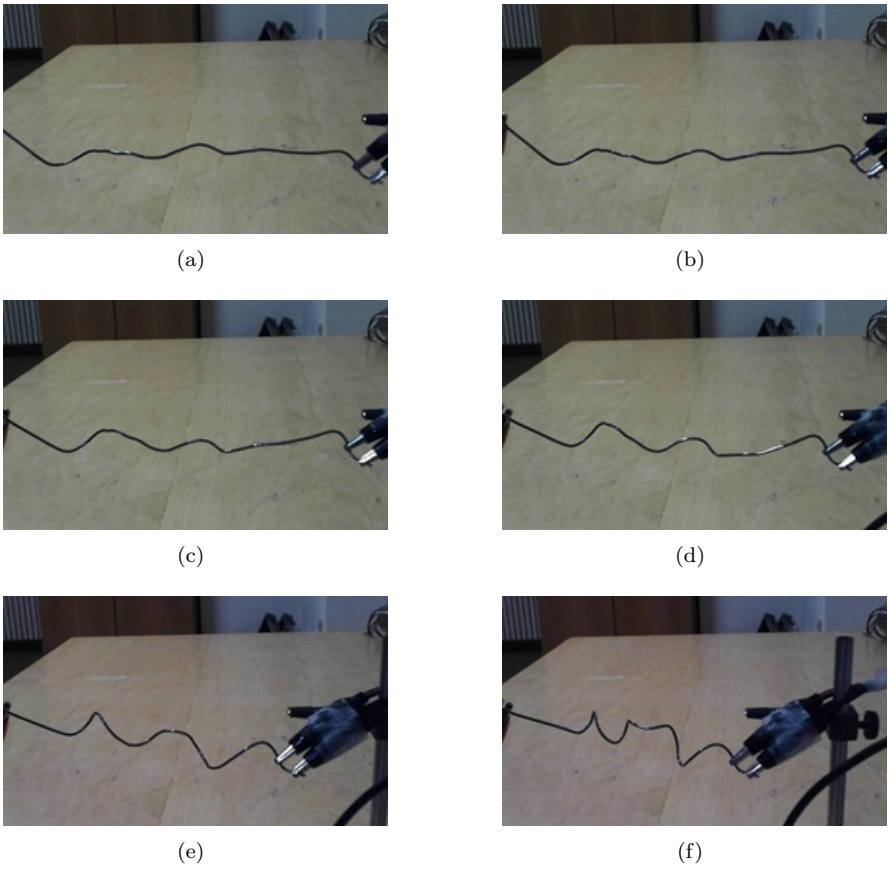

Figure 39: Free-coiling and perversion by means of SMA

In order to reproduce and mimic the grasping phase, a NiTi wire can be trained to recover a coiled shape when heated. After that, the material has been deformed end elongated. Indeed, if properly heated, the material can emulate a grasping behavior; this occurs by applying current or heating small subsequent pieces of the material from the base to the tip. It recovers step by step the memorized shape, thus works in a bio-mimetic manner.

3.4 Conclusions

The tendril capabilities to act as a linear actuator have been reproduced in this chapter by means of both a phone cord and SMA biomimetic materials. The results show how the phenomenon is reproducible even if, in case of SMA, the shape recovery capabilities fast degrade.

If SMA materials would be used for a pulling purpose, i.e. to reproduce the free-coiling phase, either a shape with perversion or a not fully stretched starting point, i.e. only an elongated spring, can be used as solutions. On the other hand, the grasping enhancing effect by means of a free-coiling phase has been recreated.

4 Phase: Bio-inspired tendril...model, simulation and emulation

Abstract. *In this phase, a robotic approach is exploited to describe and simulate a bio-inspired robotic tendril from a kinematic point of view. It is conceived by dividing the structure in two parts: one devoted to the free-coiling and the other one to the grasping. A kinematic simulator able to reproduce the three main motion phases of a tendril is implemented. Moreover, a practical realization of the GC part is presented as well as a proof-of-concept of a section for the modular structure. Finally, ideas and possible future work that can exploit the evolution of this approach are presented.*

Keywords: Tendrils, bio-robot, reflex, distributed control

4.1 Introduction: literature review

To give robots the grasping ability, mechanical hands have been studied since the eighties [62, 60].

Grasping hands are studied from different bio-mimetic points of view: tactile sensing, restraining (fixturing) and manipulating with fingers (dexterous manipulation). To this end, both the mathematical model of a grasping hand behavior and the recognition of the object form and position are complex tasks. As a consequence, robotic grasping systems usually assume as known most or all the information needed for the grasping or exploit vision to obtain relevant objects information [67, 13].

Robot mechanical hands are usually simple, without anthropomorphic intent (i.e. grippers, jaws, compliance devices), and developed to perform specific tasks (i.e. suction cups for keeping glass, compressed air-driven tongs). On the other hand, anthropomorphic multifingered grasping/fixturing can be classified in two classes: enveloping and fingertip grasp. Broad reviews on these topics can be found in [5, 68, 75].

Some natural systems show a sort of reflex-like behavior for mediating with the objects to grasp by exploiting the tactile information. On the tactile topic, from the mechatronic point of view, a lot of work has been made to create, optimize and miniaturize tactile sensors solutions [75]: resistive - with strain gauges, piezoresistors, conductive polymers, elastomer composites, conductive fluids -, capacitive, piezoelectric and optical sensors are the main classes.

From the biomimetic point of view, in particular for coiling robotics systems, some work has been done to replicate the capabilities of some special animals.

Among these and for the purpose of this project, special attention has to be paid to robotic snakes. The Hirose's group, starting from his study [25] on the snake movements, has developed a class of rigid-link hyper redundant dexterous manipulators called "active cord mechanism" (ACM) or serpentine robots. "Continuum manipulators" [58] show a backbone structure system with a high number of joints and a very short length of links to tend to an ideal continuum condition that can bend and contract/extend in any point (e.g. [9, 39]).

Tendons and artificial muscle technologies are among the most effective hardware realizations. Successful works on backbone manipulators are also the octopus and arms and tentacles of squid - inspired robots [72], e.g. the OCTARM robot, the trunks and tentacles-inspired robot [40, 73], e.g. Air-Octor.

A deep investigation has been done also in the design of endoscopes by observing the snake movements. In this regard, a lot of work can be found in literature, ([51, 1, 18]). These systems, even if not directly inspired to the tendril plant behavior, have a lot in common especially if the circumnutation phase is considered. Indeed, both for the tendril and endoscope structures, the motion shows similar movements.

Recently, the Octopus project (EU-FP7) has studied novel design principles and technologies for a new Generation of high dexterity soft-bodied robots inspired by the morphology and behavior of the octopus since 2007 [81]. The octopus tentacles are able to carry out an effective grasping by contracting and elongating muscles and fibers and bend in the desired direction.

Effective results related to the bio-mimesis of the system grasping capabilities have been recently published [12, 49, 26, 41].

Concerning the grasping and free-coiling phases based on the plant tendrils (see phases 1 and 2), to our knowledge, no biomimetic results or attempts can be found in literature. Indeed, if the grasping phase is considered, important differences or not yet discovered similarities between the plant and animal behaviour can be appreciated:

- Tendrils motion and contact recognition

  Passiflora tendrils are able to recognize supports and obstacles on the overall surface thanks to the presence of specialized fibers. Indeed, tendrils bend in different directions and not only on one side, especially in the second half of the length.

- Multiple coils

  This capability can be viewed looking at a winch-capstan system. Multiple coils allow to have a small and negligible tension in the tendril apex, to have a tension that increases from the apex to the most inner touching point and to avoid the slippage due to the increased touching surface and the related friction.

- Reflex - modular distributed behavior

  As highlighted in the 2^{nd} phase, the most sensitive part of the tendril is in its second half. When it touches or is touched in this zone, it shows a reflex behavior, i.e. it bends. The signal transmission is yet not well known even if experimental observations show a sort of modular behavior. This means that the zone that senses a support induces a contraction phase to the near fibers; after that, if the contact increases, i.e. the touched nearest zones sense a contact, the bending signal is transmitted creating the overall tendril motion and grasping.

  Thanks to this, a distributed reflex control is made, allowing the activation of the motion locally and only when necessary. This is surely an advantage from an energetic point of view since the modules “sleep” in a normal phase and are activated only when necessary.

The circumnutation phase, in which all the tendril moves, is a manifestation of the radially asymmetric growth rate and results in a sweep "seeking" movement that can, for our biomimetic purposes, be simplified in a motion created by actuating the tendrils base.

Moreover, if the free-coiling phase is considered, other important features can be highlighted:

- Enhanced hook for support radius over the limits;

  As underlined in Phase 2, when the radius of the support to be coiled is greater than a certain limit, the coiling phase is not possible but the grasping occurs by means of a hook development which capabilities are enhanced through the free-coiling phase.

- Spring actuator

  The free-coiling phase allows to pull the stem towards the grasped support. By coming back to the original/intrinsic helical shape, the tendril shortens the distance between the fixed end-points. Moreover, the helical-spring shape is perfectly tuned to resist to external loads and disturbances.

Thus, different and better characteristics induce us to evaluate and investigate how to mimic the plant tendril system structure.

4.2 Kinematic Model

In order to design a bio-robotic tendril, the overall structure has been considered from a kinematic point of view. The model has been conceptualized and simplified dividing the tendril in two main parts: the first (FC) mainly devoted to the free-coiling and pulling phase, and the second (GC) devoted to the coiling and grasping phase (Fig. 40).

(a) (b)

Figure 40: Bio-mimetic tendril model: GC and FC modules

Thanks to this, the GC part, devoted to the grasping, can be subdivided in independent modules able to react when in touch or hit by something, and bend; the FC part, devoted to the pulling, can be viewed as a single actuator that changes its shape from a linear wire to a helical spring. To model the GC part, the approach followed by Jones and Walker [39, 40] and Hannah and Walker [23], has been chosen. They worked on the kinematics of multi-section continuous robots. In this way, a kinematic description can be associated at each sub-section by means of elementary pairs/joints, a description with the Denavit-Hartenberg (DH) notation, and a reflex modular motion. Moreover, a direct relation between a "classical DH" section and a wire driven module can be defined allowing to compute the cable tensions for a particular sub-section motion.

The idea is to fully model the kinematics of the tendril GC part using closed-form equations. This is carried out by dividing it in sections/modules which can at least bend in two dimensions.

4.2.1 Modular structure: GC part

The GC part has been considered as subdivided in n-sections.

Kinematics involves two main steps: first, the GC tendril kinematic problem is approached by means of a series of substitutions applied to a modified homogeneous transformation based on the Denavit-Hartenberg (DH) notation; second, velocity kinematics could be solved by computing the Jacobian for each and then by chaining them together.

The main assumption is that the tendril section has a constant curvature. The forward kinematics of a robotic system is usually computed by a standard homogeneous transformation matrix $\boldsymbol{A}(\theta,\boldsymbol{d})$ based on a DH table parameters; it allows to transform the independent degrees of freedom $(\theta,\boldsymbol{d})$ in task coordinates, i.e. position and orientation of the end-effector.

A tendril-based continuous robot lacks joints and each tendril section can be viewed and modeled through an arc of constant curvature, i.e. by means of parameters such as length, curvature and/or angle of curvature.
To shift between this formulation and a conventional DH formulation, an equivalent rigid-link-joint section and the transformation relations have to be defined; thus, to fit a conventional rigid-link manipulator to the tendril section, the relationship $[\theta, \boldsymbol{d}]^T = f\ (l, \kappa,\ \varphi)$, where θ and $\boldsymbol{d}$ are the DH parameters, l the length section, κ the curvature and φ the angle of curvature (see Fig. 41), has to be found.

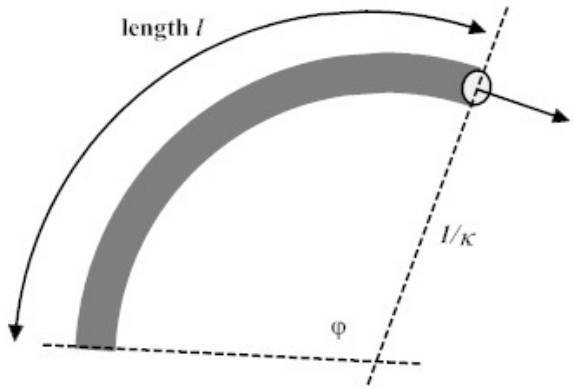

Figure 41: Tendril section: geometry and parameters

Once defined the relations, in order to simulate the tendril movement and grasp behavior, the target is to relate position and orientation of each section and of the tendril tip to the joint parameters.

For each section, a simplified robotic system made of rigid links and joints is defined. Fig. 42 shows the "equivalence" between the real wire/tendril section and the robotic-tendril.

The section is composed of a first universal joint, i.e. two revolute pairs with orthogonal and intersecting axis of rotation, followed by a prismatic joint, and ended with a second universal joint; this last joint and the related variables are coupled with those of the first pair of the following section.

The first pair allows to rotate the local frame axis to be oriented to the section tip, the prismatic joint allows the translation to the last point of the section, i.e. the final coordinate frame origin, and the last pair allows to correctly rotate and orient the local frame with the following section.
Since the last pair of a section and the first pair of the following are coupled, the independent variables result in three per section. Regarding the prismatic joint, if the number of sections is sufficiently high, it can be considered as fixed, i.e. constrained, since the error made becomes negligible.

The DH table, Tab.3, can be defined after the definition of the local coordinate frames through the DH notation. The fixed rotation on the x-axis at the beginning of the DH table is added to have the section extension along the z-axis; the fixed rotation at the end of the DH table allows to correctly orient the tip.

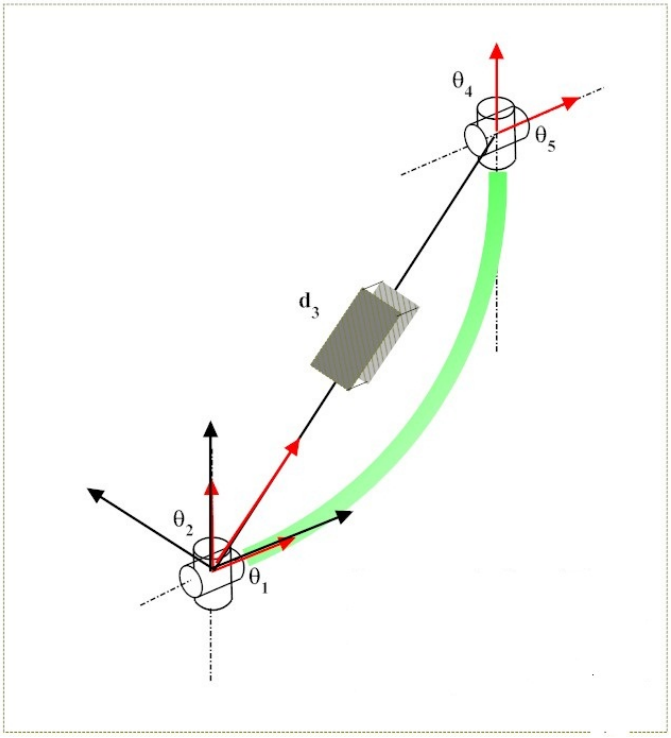

Figure 42: Tendril section: equivalence wire - robot

The resulting homogeneous transformation matrix for each section of the GC part is:

$$\mathbf{A} = \left[\begin{array}{ccc|c} -c_1 s_2 s_4 c_5 + c_1 c_2 c_4 c_5 - s_1 s_5 & c_1 s_2 s_4 c_5 + c_1 c_2 c_4 s_5 - s_1 c_5 & -c_2 s_4 c_1 + s_2 c_4 & c_1 c_2 d_3 \\ -s_1 s_2 s_4 c_5 + s_1 c_2 c_4 c_5 - c_1 s_5 & s_1 s_2 s_4 s_5 + s_1 c_2 c_4 s_5 - c_1 c_5 & -s_1 c_2 s_4 + s_2 c_4 & s_1 c_2 d_3 \\ (c_2 s_4 + s_2 c_4) s_5 & -(c_2 s_4 + s_2 c_4) s_5 & c_2 c_4 + s_2 s_4 & s_2 d_3 \\ 0 & 0 & 0 & 1 \end{array}\right]$$

where $c_i = \cos(\theta_i)$ and $s_i = \sin(\theta_i)$.

The geometrical transformation between the DH parameters and the parameterization of the tendril as a spatial curve, i.e. l,κ ,φ , can be found by looking at the geometry of a tendril section (Fig. 43).

Since the hypothesis of constant curvature has been adopted, each tendril section can be considered/viewed in a 2-D plane π with respect to which its coordinates

Table 3: DH table for a tendril section

Link	a	α	d	θ
-	0	$\pi/2$	0	0
1	0	$\pi/2$	0	θ_1
2	0	$\pi/2$	0	$\theta_2 + \pi/2$
3	0	$-\pi/2$	d_3	0
4	0	$-\pi/2$	0	$\theta_4 + \pi/2$
5	0	0	0	θ_5
-	0	$-\pi/2$	0	0

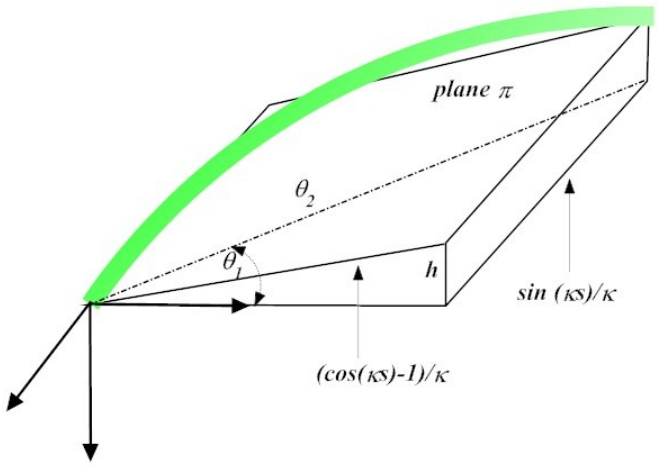

Figure 43: Tendril section geometry

are:

$$(x, y)_\pi = (cos((\frac{\kappa s - 1}{\kappa})), sin(\frac{\kappa s}{\kappa}))$$

These coordinates correspond, in the rototranslation matrix $\boldsymbol{A}$, to the translational terms in the first and second row of the fourth column. The distance d between the extreme points of the tendril section can be found as:

$$d = \frac{2}{\kappa} sin(\frac{\kappa s}{2})$$

Now, thanks to geometrical and trigonometric identities, the system can be solved and the independent variables computed. It holds:

$$\theta_1 = tan^{-1}(\frac{-1}{tan(\frac{\kappa s}{2} cos(\varphi))})$$

$$\theta_2 = sin^{-1}(sin(\frac{\kappa s}{2}) sin(\varphi))$$

Since the distance between the extreme points of the section is d_3 and the last two rotations restore the initial orientation, i.e. repeat the rotations of 1 and 2 in the reverse order, the relationship between the tendril curve and the robotic formulation results:

$$\begin{bmatrix} \theta_1 & \theta_2 & d_3 & \theta_4 & \theta_5 \end{bmatrix}^T = \begin{bmatrix} tan^{-1}(\frac{cos(\frac{\kappa s}{2})}{-sin(\frac{\kappa s}{2})cos(\varphi)}) \\ sin^{-1}(sin(\frac{\kappa s}{2} sin(\varphi))) \\ \frac{2}{\kappa} sin(\frac{\kappa s}{2}) \\ sin^{-1}(sin(\frac{\kappa s}{2}) sin(\varphi)) \\ tan^{-1}(\frac{cos(\frac{\kappa s}{2})}{-sin(\frac{\kappa s}{2})cos(\varphi)} + \pi) \end{bmatrix}$$

Finally, also the rototranslation matrix can be expressed in equivalent manner with respect to the "curve" parameters:

$$\mathbf{A} = \left[\begin{array}{ccc|c} cos^2(\varphi)(cos(\kappa s)-1)+1 & sin(\varphi)cos(\varphi)(cos(\kappa s)-1) & -cos(\varphi)sin(\kappa s) & \frac{cos(\varphi(cos(\kappa s)-1))}{\kappa} \\ sin(\varphi)cos(\varphi)(cos(\kappa s)-1) & cos^2(\varphi)cos(\varphi)(cos(\kappa s)-1) & -sin(\varphi)sin(\kappa s) & \frac{sin(\varphi(cos(\kappa s)-1))}{\kappa} \\ cos(\varphi)sin(\kappa s) & sin(\varphi)sin(\kappa s) & cos(\kappa s) & \frac{sin(\kappa s)}{\kappa} \\ 0 & 0 & 0 & 1 \end{array}\right]$$

By simplifying the system and supposing a planar 2-D motion, the curve is planar with a constant curvature. It can be associated to a planar robotic system made of two revolute joints with axis of rotation perpendicular to the plane, linked with a prismatic joint. In such a case, the DH table results as in Tab. 4 and the rototranslation matrix as follows:

Table 4: DH table for a tendril planar section

Link	a	α	d	θ
1	0	-$\pi/2$	0	θ_1
2	0	$\pi/2$	d_3	0
3	0	0	0	θ_5

$$\mathbf{A} = \left[\begin{array}{ccc|c} cos(\kappa s) & -sin(\kappa s) & 0 & \frac{cos(\kappa s)-1}{\kappa} \\ sin(\kappa s) & cos(\kappa s) & 0 & \frac{sin(\kappa s)}{\kappa} \\ 0 & 0 & 1 & 0 \\ 0 & 0 & 0 & 1 \end{array}\right]$$

4.2.2 Modular structure: FC part

The FC part can be adequately modeled by a unique kinematic section. Indeed, on one hand it is constrained by the stem/fixed base and, on the other hand, to the contact/grasping point.

The chosen section has the same characteristics of the previous defined ones, both for the 3D and 2D motion. Indeed, thanks to the first universal joint the tendril can be properly oriented; the prismatic joint allows to consider the free-coiling main effect, and the second universal joint to take into account the correct final orientation for connecting the two bio-mimetic tendril parts. Since the two extreme points are constrained and no torsion has to be allowed for both the base and the connection with the GC part, the two universal joints are passive joints; this means that the related angular values are defined once ended the grasping phase. The unique active joint is the prismatic pair; its length value is the distance between the base and the origin of the first local coordinate frame of the GC section.

From the kinematic point of view, the problem consists in a shift of point of view: the end-effector of the section becomes the point connected with the base, the stem, and the movement has to be described with respect to the local reference frame of the last pair of the section, i.e. the one that now is constrained and fixed (see Fig.44).

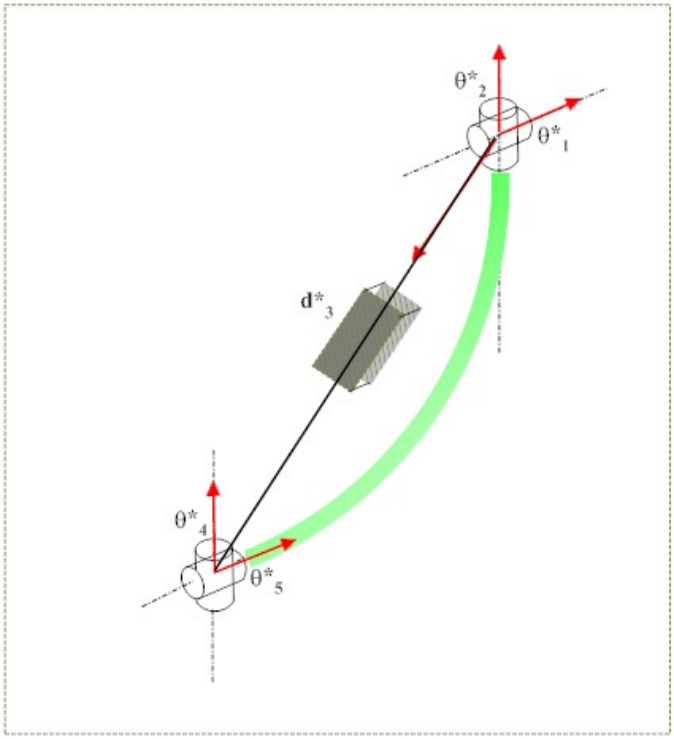

Figure 44: Tendril free-coiling section kinematics

4.3 Simulation

The derived formulas have been implemented in a Matlab simulator to simulate the kinematics of a bio-inspired tendril.

The FC section has been defined with a greater length with respect to the GC sections, e.g. half of the overall length, and considered in the searching and grasping phase constrained in its origin point.

The GC section has been divided in n sections of equal length.

The circumnutation phase has been simplified and implemented as a centralized motion by driving the first universal joint of the chain; this means that the overall tendril spans a cone in a 3D motion (or an angle in 2D) searching a support to be grasped (Fig. 45).

The grasping phase has been conceived as a reflex behavior considering, for this purpose, each GC section as an independent module. The 3^{rd} joint has been considered as fixed in length since a large number of sections are simulated. This means that, if a GC section touches an obstacle, it stops the main circumnutation motion; after that, it reacts by actuating the last joint of the section in the direction of the stimulus. This results in bending the remaining tendril in the stimulus direction until when either another section recognizes a stimulus, i.e. is in touch with the support, or the minimum curvature angle is reached. In the former case the bending motion continues and the grasping by coiling goes on; in the latter case the motion stops and the tendril motion has to be zeroed/restarted (Fig.s46,46(f)).

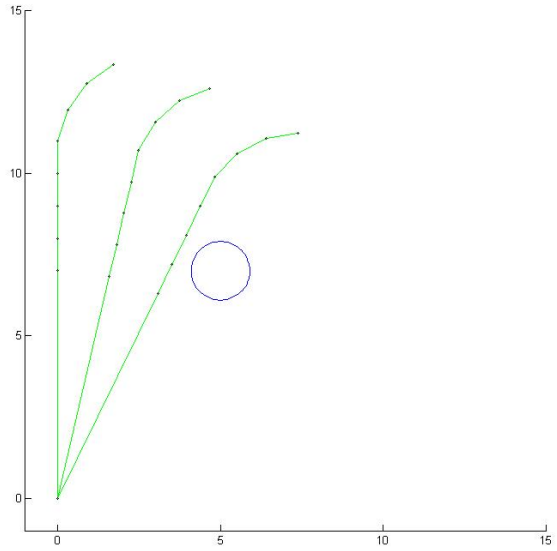

Figure 45: Biomimetic tendril kinematics: circumnutation; only the 1^{st} joint and the 1^{st} section are actuated

The contact has been implemented by searching for each module if there is intersection between the segment that connects the two universal/revolute joints, i.e. d_3, and the surface to be find, e.g. a cylinder (Fig. 46).

The FC behavior has been implemented as a pulling motion driven by the prismatic joint. In such a case, the base of the section becomes the connection point between the GC and FC parts, while the end-effector becomes the coordinate frame of the stem (Fig.47).

Three main behaviors can be thought for the grasping and pulling activity:

1. "growing" the system. In this case, if the stem is considered as a linear guide that can move on the vertical axis, the FC behavior, by shortening the distance between the two limit points, allows to move this prismatic joint and, thus, to extend the stem (Fig. 48(a));
2. pulling a load. In this case, the FC activity works to move a load in a predefined direction (Fig. 48(b)).
3. holding the stem under external loads, i.e. wind; In such a case, once the FC part has created a helical spring and an equilibrium point is found, such a spring allows to stand external loads and have a robust grasping.

From another point of view, the GC part can be considered as a unique section. This can be made to describe, from a kinematic point of view, the relation between a particular curvature and the equivalent robotic module. Indeed, if the d_3 is not fixed and starts from its maximum extension, by shortening this linear joint, since the overall real-tendril length is constant, a particular curvature is represented (Fig.

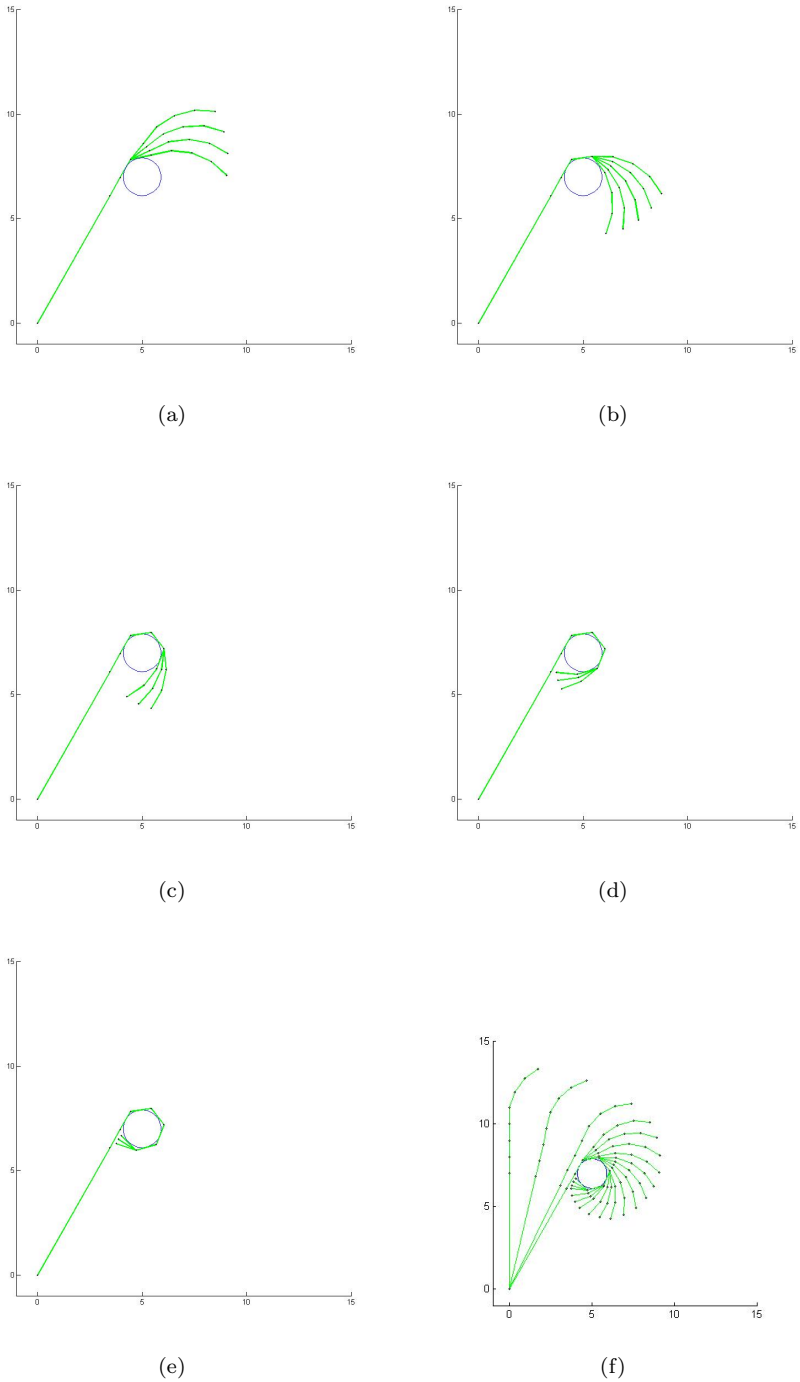

Figure 46: Bio-mimetic tendril kinematics: grasping

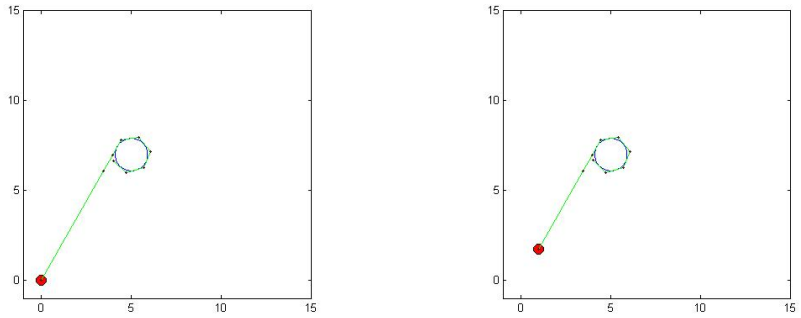

(a) (b)

Figure 47: Bio-mimetic tendril kinematics: free-coiling

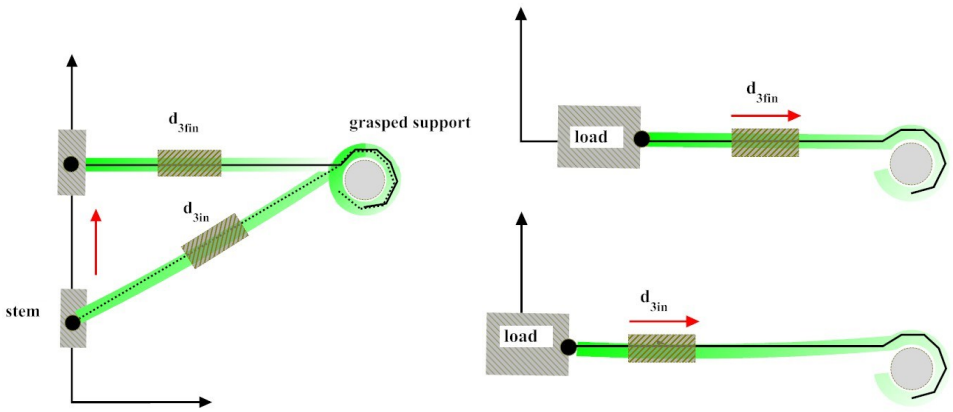

(a) (b)

Figure 48: Free-coiling behavior ideas

49). This is useful if a kinematic description and simulation is associated to a unique GC section prototype.

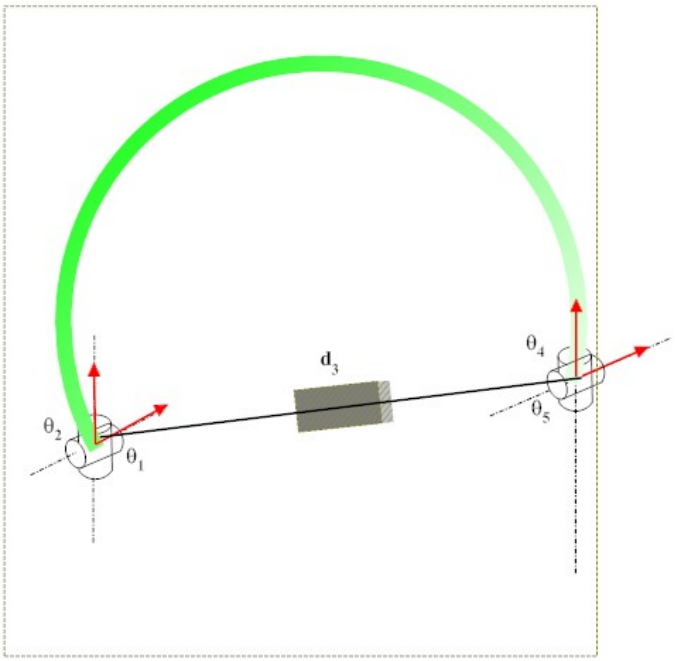

Figure 49: GC unique section kinematics

4.4 From rigid links to wires

The kinematic definition by means of universal/revolute and prismatic joints will result, if a large number of sections is considered, in a large number of joint sensors and actuators. Moreover, the classical target in continuous and modular robots is to determine and know the robot shape. In our case, the idea is to conceptualize a bio-mimetic tendril that searches a contact by actuating only one joint and each section is driven and bends only by a reflex behavior. Thus, the shape determination is not so important or, at least, precise information for all the sections is no required. Hoverer, to create and simulate an effective system, it is important to take into account the overall direct kinematics and all the actuated joint values. In order to move to a bio-mimetic tendril prototype driven by SMA materials and a lightweight cable or spring (in the following we will use the term "wire") driven system, a transformation between the developed kinematics and the cable length variables has to be defined.

By maintaining the assumption that each section bends with a constant curvature and considering for simplicity a planar motion, hence a 2D system, each section can be evaluated.

Given the simplified drawing of the section in Fig. 50, the realization idea can be described as: the section is based on a revolute joint composed of two rigid elements with same geometrical dimensions. By naming w and h the width and the height of the two rigid elements, wl_i the length of the i-th wire (i = 1 or 2), the wire and system kinematics can be computed.

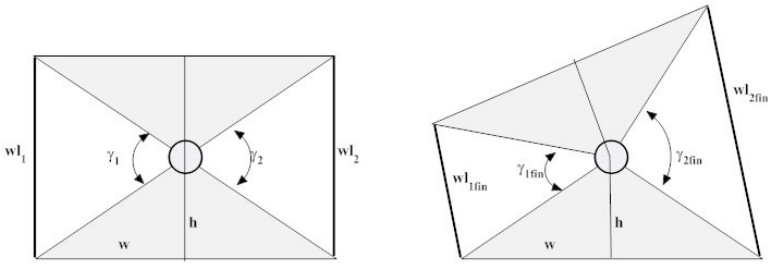

Figure 50: Planar section model driven by wires

w and h create a right-angle triangle. After the actuation of one of the wires, the final wire length results wl_{if}=wl_i*(fin)* and the length variation, considering for instance the wire 1, can be described as:

$$\Delta wl_1 = wl_1\,(fin) - wl_1\,(in) = wl_{1f} - wl_{1in}$$

The angle γ_1, controlled by the wire lengths, changes from γ_{1in} to γ_{1fin} and, in this final configuration, it is:

$$\gamma_{1fin} = atan(\frac{\sqrt{4d^2 - (2d^2 - wl_{1f}^2)^2}}{2d^2 - wl_{1f}^2})$$

with d the hyphotenuse of the right-angle triangle with w and h catheti.

The revolute joint rotation can be computed considering that the sum has to be 180°; it holds:

$$\varphi = \pi - 2atan(\frac{w}{h}) - \gamma_{1fin}$$

Regarding the second wire, the angle that defines its final length is:

$$\gamma_{2fin} = \pi - 2atan(\frac{w}{h}) + \varphi$$

Thus, the wl_2*(fin)* can be computed as:

$$wl_2\,(fin) = 2\sqrt{h^2 + w^2}sin(\gamma_{2fin})$$

If a SMA material is adopted, the Δwl_i is driven by heating the material and, hence, by applying current. In such a case the final length wl_{if} can be considered as constant, i.e. the contracted length when SMA is heated.

The relation between the DH parameters and the wire lengths can be computed (look at Fig.51) by exploiting geometrical relations.

Given the φ angle, it is possible to find the value of β and α; it holds:

$$\beta = \frac{\pi - \varphi}{2}$$

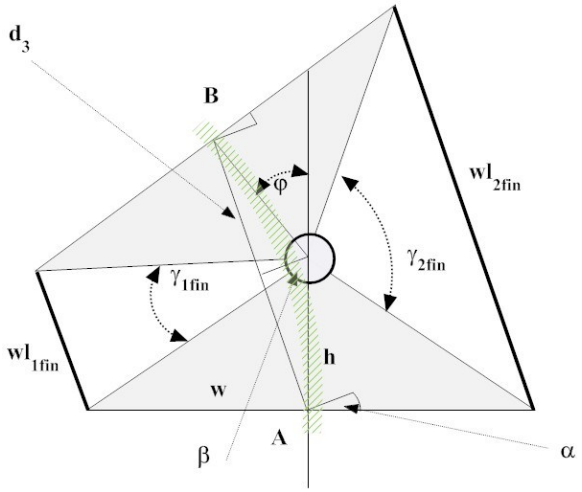

Figure 51: Section geometry and DH variables

$$\alpha = \frac{\pi}{2} - \beta$$

The distance between the two main frames, i.e. d_3, is the distance between **A** and **B**:

$$d_3 = 2hsin(\beta)$$

In such a way the direct relation between the wire lengths and the DH parameters is found.

4.5 Proof of concept

Two main strategies have been evaluated in order to physically reproduce the tendril coiling behavior.

In the first case, the idea has been to work with a GC part made of a unique module actuated by SMA wires.

In the second case, the idea has been to evaluate a modular structure, hence a GC part made of many sections, and try to design a hardware realization of one section by exploiting the properties of the SMA materials.

4.5.1 GC part: single section

In this attempt, we tried to replicate the coiling behavior of a tendril by means of SMA materials.

The idea is to properly actuate NiTi wires and create a simple, light and small structure able on one hand to bend and coil and, on the other hand, to recover a straight or almost linear shape.

To this end, SMA NiTi wires of the same length, e.g. 100 [mm], have been used; to some of them a coiled shape has been memorized while the remaining have been trained to recover a straight shape when heated.
In such a way, by alternatively giving current to the "straightened-if-heated" circuit or to the "coiled-if-heated" circuit, Fig.52, the bending and coiling behavior of the tendril can be properly emulated.
The amount of current that has to flow within the wires directly depends on the geometrical dimensions, on the mechanical and physical properties of the material and on the velocity of actuation that is searched. Indeed, the greater the current flowing in the SMA wires, the faster the changing phase temperature is reached and the motion created.

Fig.s 53 and 54 show some experimental tests that show the goodness of the approach.

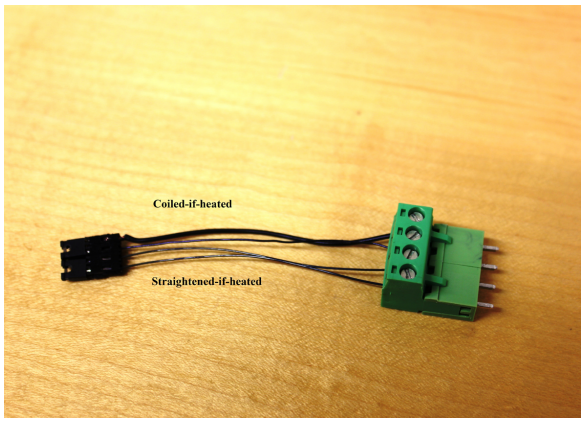

Figure 52: GC unique section simple prototype

4.5.2 Multi-section GC part: section prototype

As described previously, the GC section kinematics can be associated to a wire-driven system. In particular, if a 2D section is considered, the kinematic solution previously carried out can be exploited to design a possible proof of concept.
Taking into account that SMA materials can shorten in their "active" condition, they can act as actuators and change the orientation of the superior platform. In such a manner, the section bends in the wanted direction. In order to recreate the wires, two main roads have been considered: either to exploit Flexinol^{TM} wires or NiTi springs.
In the former case, the wires do not show a large contraction (e.g. 3-5 % of their lenght) and they return to the un-shortened state if the current is leaved out. In the latter case, the springs act as a linear actuator and with a large force; after being heated, they almost remain in the final state if no counteracting force is applied.

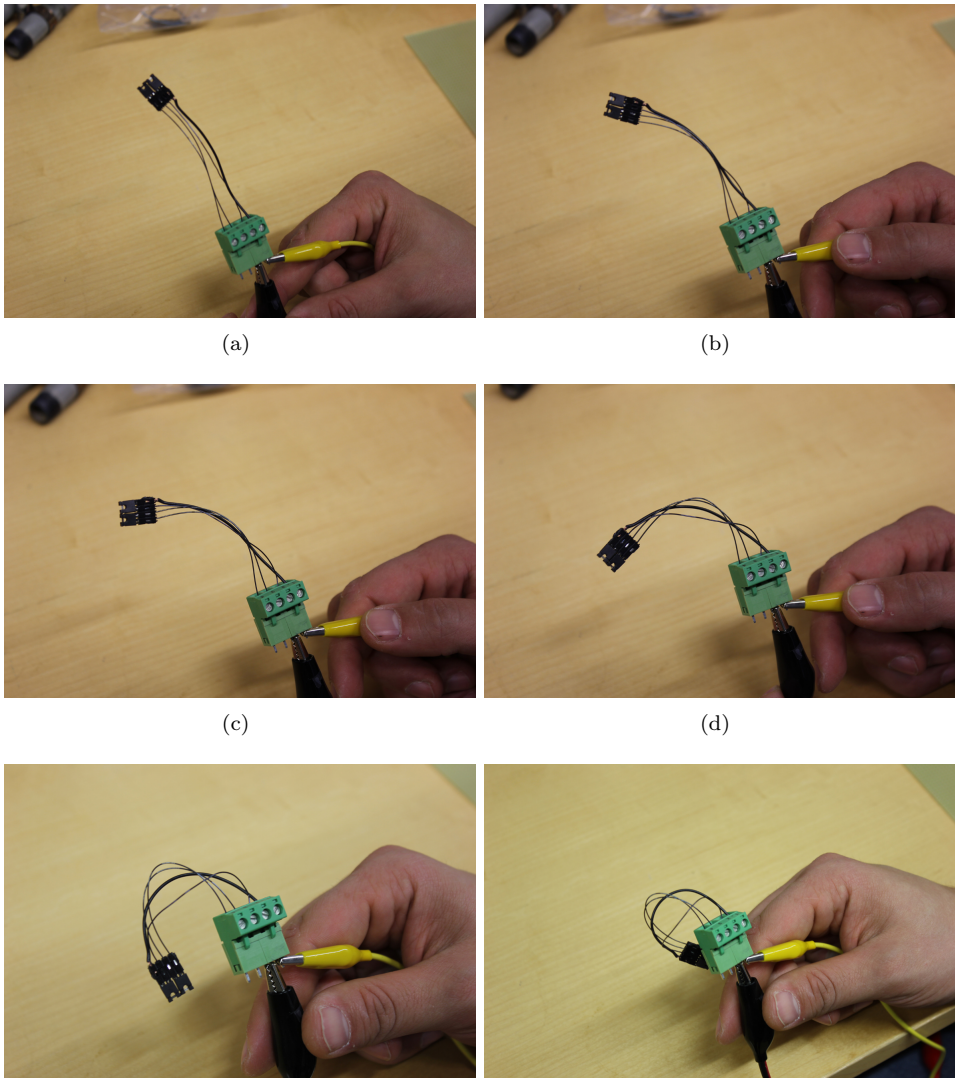

(a) (b)

(c) (d)

(e) (f)

Figure 53: Test 1: coiling

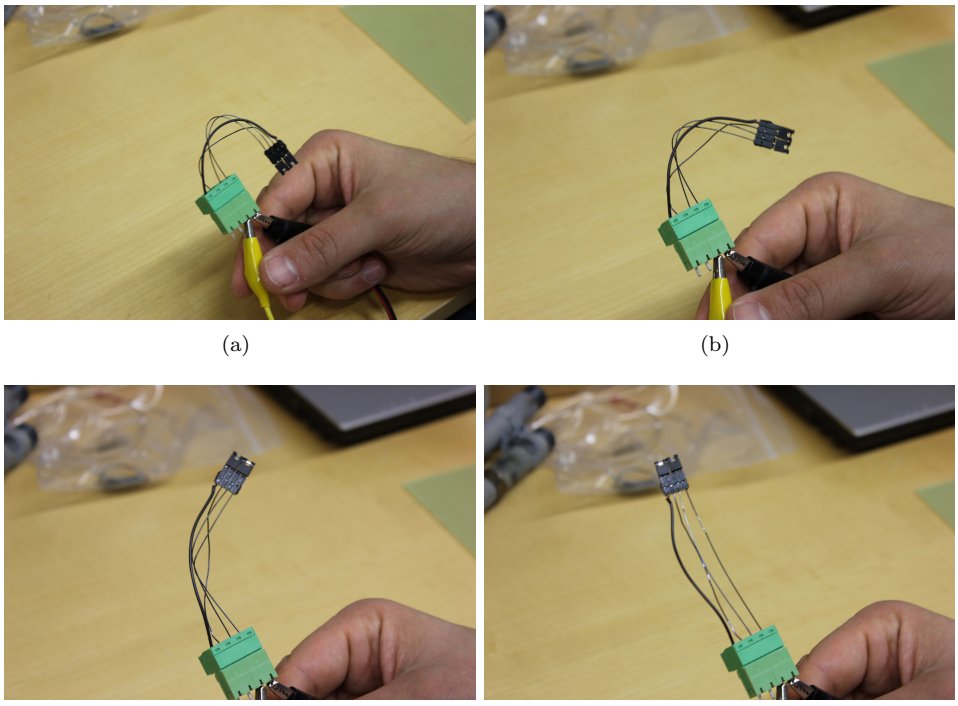

(a) (b)

(c) (d)

Figure 54: Test 2: straightening

Preliminary tests have been made with NiTi helical springs which main characteristics are: diameter 750 [μm], length when heated 29 [mm], external diameter 6 [mm],wire diameter 750 [μm], transition temperature 45-55°C, Fig.55.

Figure 55: NiTi helical compression spring

These springs can be easily elongated (maximum length 140 [mm]) and, when current is given and the transition phase temperature is reached, they contract to the compressed helical spring length. By choosing such kind of actuator, it is possible to design different kind of modules.
In Fig.56, the 3D view of a planar motion section driven by counteracting springs is shown. In this case, if the two helical springs are mounted in an elongated configuration, i.e. compressed length plus a displacement. Once a wire is driven, the module bends in the contracted helical spring direction thanks to the hinge; in the meantime, the spring not actuated elongates to reach an equilibrium point. In the described configuration, considering that at the end of the active phase one spring is contracted and the final configuration is almost retained, the overall module has bent with a certain angle, thus a tendril-like motion is replicated.

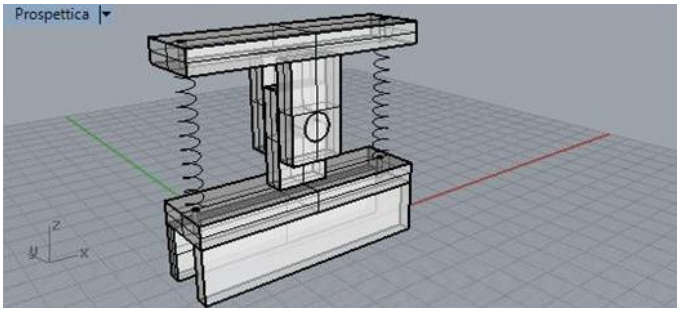

(a)

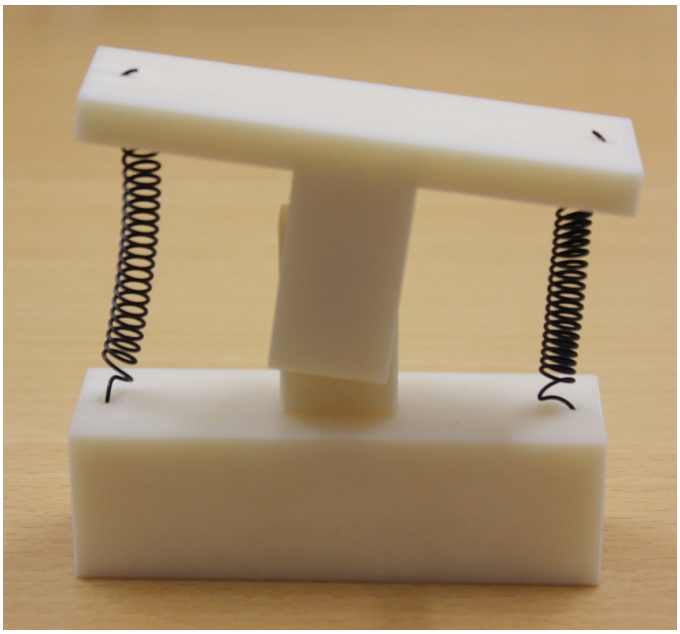

(b)

Figure 56: Two helical spring section: a) 3D design; b) ABS prototype

If a unique bending side is searched, a system as in Fig. 57 can be exploited. Both the wires are made of SMA materials. On the bending side, the rest state shows, as previously, a spring in an elongated configuration; on the other side, the spring in the contracted configuration, i.e. l_0, is mounted. Thanks to this, when the first spring is heated, it contracts and bends the module; in the meantime, the second spring elongates of a fixed amount. Then, if the first wire is leaved cold and the second wire is get hot, the "zero" state is re-gained.

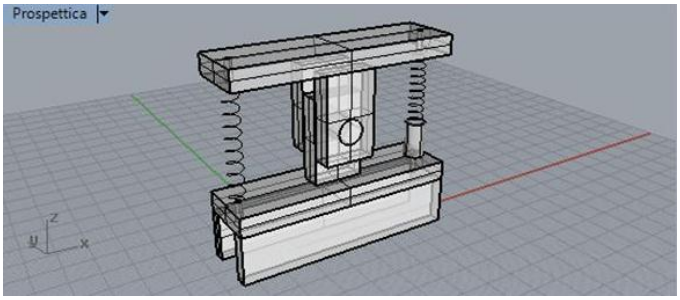

Figure 57: Two helical spring one-direction section

Same considerations and designs can be made if cables are considered (Fig. 58). In this case, if cables such as Flexinol^{TM} are exploited, the main drawback results in the rest state, i.e. when the material is not in the on-state. Indeed, when the voltage is cut-off, the temperature in the material lowers under the transition threshold and the material goes back to the original elongated state. In this condition, the bent position can be maintained only if the on-state is retained, i.e. by applying voltage and consuming energy. Since the variation in length of such materials is quite low, e.g. 5 %, devices to double and multiply the contraction can be evaluated (Fig.59).

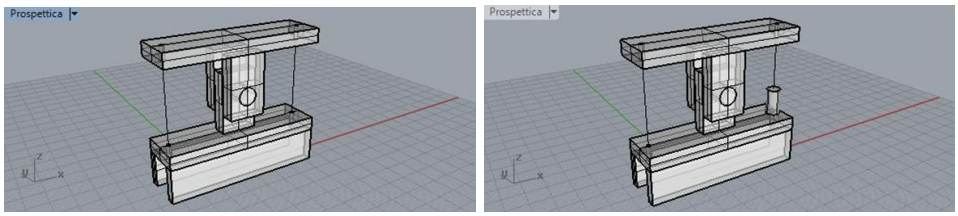

(a) (b)

Figure 58: Two cables section: a) direct connection; b) one-direction

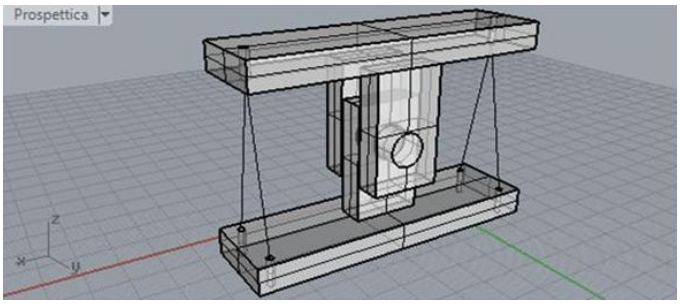

Figure 59: Two cables section: multiplied contraction

4.6 Conclusions and future work

The results and directives of the first three phases have been exploited to model and design a bio-inspired robotic tendril. Starting from the state of the art in grasping systems and/or continuous bio-inspired robots, the main differences between the tendril structure, behaviors and the available literature have been highlighted. After that, a tendril-like structure has been conceptualized and simplified by splitting the system in two main parts: the first, attached to the base to be moved, that is devoted to the free-coiling pulling activity, and the second, the sensible part of the tendril, devoted to the main grasping activity.

The bio-inspired tendril model has been developed from a kinematic point of view and the relations between the active parameters found. The DH notation has been used to describe each section of the system. The relation between the robotic model, i.e. revolute and prismatic joints, and its equivalent wire-based system, has been computed in view of a SMA use.

Two different designs for replicating the grasping behavior by means oF SMA materials have been proposed. Both cables and springs have been considered as solutions.

The simulations and results show that the ideas are effective and the tendril behavior reproducible.

Possible future work should focus the exploitation of the designed systems for creating new systems such as:

- legged and climbing robots able to grasp by means of the coiling effect and climb by means of the free-coiling behavior;
- linear one-shot free-coiling autonomous actuators. This means that the free-coiling helical spring shape will use the transition phase of the SMA materials for bringing near two parts only by heating the material. With respect to simple wires the helical spring shape ensures better performances.

A Appendix

Photos, time lapses and videos can be found in a separate folder.

References

[1] J Abadie, N Chaillet and C Lexcellent, *Modeling of a new SMA micro-actuator for active endoscopy applications*, Mechatronics 19: 437-442, 2009

[2] Y Bar-Cohen, *Biomimetics Nature-Based Innovation*, CRC press, Taylor and Francis Group, 2012

[3] M Bergou, M Wardetzky, S Robinson, B Audoly, E Grinspun, *Discrete elastic rods*, Journal ACM Transactions on Graphics (TOG) - Proceedings of ACM SIGGRAPH, 27:3, Article No. 63, August 2008.

[4] CA Beveridge,EA Dun, C Rameau, *Pea has its tendrils in branching discoveries spanning a century from auxin to strigolactones.* Plant Physiol. 151: 985–990, 2009

[5] A Bicchi and V Kumar, *Robotic grasping and contact: a review*, Proceedings of IEEE International Conference on Robotics and Automation, 2000, ICRA '00, 1, 348 - 353, San Francisco, CA , USA , 2000

[6] J Braam, *In touch: plant responses to mechanical stimuli*, New Phytologist, 165: 373-389, 2005.

[7] AH Brown. *Circumnutations: from Darwin to space flights*, Plant Physiol 101:345-8, 1993.

[8] AJ Bowling and KC Vaughn, *Gelatinous fibers are widespread in coiling tendrils and twining plants*, American Journal of Botany 96(4): 719-727, 2009.

[9] R Buckingham, *Snake arm robots*, Ind. Robot Int. J. 29(3), 242-245, 2002.

[10] R Budynas and K Nisbett, *Shigley's Mechanical Engineering Design*, Mc Graw Hill, ISBN-13: 978-0073529288, 2010.

[11] V Bundhoo, E Haslam, B Birch, EJ Park, *A Shape Memory Alloy-based Tendon-driven actuation system for biomimetic artificial fingers, Part I: Design and Evaluation*, Cambridge University Press, Robotica, 2008.

[12] M Calisti, M Giorelli, G Levy, B Mazzolai, B Hochner, C Laschi and P Dario, *An octopus-bioinspired solution to movement and manipulation for soft robots*, Bioinsp. Biomim. 6, 036002, 2011

[13] G Cannata and M Maggiali, *An embedded tactile and force sensor for robotic manipulation and grasping*, Humanoid Robots, 5th IEEE-RAS International Conference, 2005.

[14] CMS Carrington and J Esnard, *Kinetics of thigmocurvature in two tendril-bearing climbers*, Plant, Cell and Environment,) 12, 449-454, 1989.

[15] C Darwin, *On The Movements and Habits of Climbing Plants*, London: John Murray, 1865.

[16] C Darwin, *The movements and habits of climbing plants*, Appleton, New York, New York, 1876.

[17] C Darwin and F Darwin, *The power of movements in plants*, Appleton, New York, New York, 1880.

[18] V De Sars, S Haliyo and J Szewczyk, *A practical approach to the design and control of active endoscopes*, Mechatronics 20: 251-264, 2010

[19] J Engelberth ,*Mechanosensing and signal transduction in tendrils*, Adv. Space Res. Vol. 32, No. 8, pp. 1611-1619, 2003.

[20] SJ Gerbode, JR Puzey, AG McCormick, L Mahadevan, *How the cucumber tendril coils and overwinds*, Science, vol. 337, August 2012.

[21] A Goriely and S Neukirch, *Mechanics of Climbing and Attachment in twining plants*, Physical Review Letters, 97, 184302 1-4, 2006.

[22] A Goriely and M Tabor, *Spontaneous Helix Hand Reversal and Tendril Perversion in Climbing Plants*, Physical review letters, 80, 7, 16 February 1998.

[23] MW Hannan and ID Walker, *Kinematics and the Implementation of an Elephant's Trunk Manipulator and other Continuum Style Robots*, Journal of Robotic Systems, 20: 45-63, 2003

[24] DJ Hartl, DC Lagoudas, *Characterization and 3-D modeling of Ni60Ti SMA for actuation of a variable geometry jet engine chevron*, in: Proc. SPIE, Smart Struct. Mater., 2007

[25] S Hirose, *Biologically inspired robots*, Oxford Univ. Press, Oxford 1993

[26] JP Hou, RHC Bonser and G Jeronimidis, *Design of a Biomimetic skin for an octopus- inspired robot- Part I: Characterising octopus skin*, Journal of Bionic Engineering, 8: 288-296, 2011

[27] S Isnard, AR Cobb, NM Holbrook, M Zwieniecki and J Dumais, *Tensioning the helix: a mechanism for force generation in twining plants*, Proc. R. Soc. B. 276, 2643-2650, 2009, doi:10.1098/rspb.2009.0380

[28] S Isnard and W. Silk, *Moving with climbing plants from Charles Darwin's time into the 21st century*, American Journal of Botany 96(7): 1205-1221, 2009.

[29] MJ Jaffe and AW Galston, *Physiological studies on Pea tendrils. I Growth and coiling following mechanical stimulation*, Plant Physiol., 41,1014-1025, 1966.

[30] MJ Jaffe and AW Galston, *Physiological studies on Pea tendrils. II The role of light and ATP in contact coiling*, Plant Physiol., 41,1152-1158, 1966.

[31] MJ Jaffe and AW Galston, *Physiological studies on Pea tendrils. III ATPase Activity and Contractility Associated with Coiling*, Plant Physiol., 42,845-847, 1967.

[32] MJ Jaffe and AW Galston, *Physiological Studies on Pea Tendrils. IV Flavonoids and Contact Coiling*, Plant Physiol., 42,848-850, 1967.

[33] MJ Jaffe and AW Galston, *Physiological Studies on Pea Tendrils. V Membrane Changes and Water Movement Associated with Contact Coiling*, Plant Physiol., 43,537-542, 1968.

[34] MJ Jaffe and AW Galston, *The physiology of tendrils*, Annu. Rev. Plant. Physiol. 19:417-434, 1968.

[35] MJ Jaffe, *Physiological Studies on Pea Tendrils. VI The characteristics of sensory perception and transduction*, Plant Physiol., 45, 756-760, 1970.

[36] MJ Jaffe, *Physiological Studies on Pea Tendrils. VII Evaluation of a technique for the asymmetrical application of ethylene*, Plant Physiol., 45,631-633,1970.

[37] MJ Jaffe, *Experimental separation of sensory and motor functions in pea tendrils*, Science 195(4274):191-2 (1977), PMID 17844039

[38] A Johnsson, *Circumnutations: Results from recent experiments on Earth and in space*, PLANTA 203: S147-S158, 1997.

[39] BA Jones, ID Walker, *Kinematics for Multisection Continuum Robots*, IEEE Transaction on Robotics, 22:1, Feb 2006

[40] BA Jones, ID Walker, *Practical Kinematics for Real-Time Implementation of Continuum Robots*, IEEE Transaction on Robotics, 22:6, Dec 2006

[41] R Kang, DT Branson, E Guglielmino and DG Caldwell, *Dynamic Model and Control of a Multiple Continuum Arm Robot Inspired by Octopus*, In Computers and Mathematics with Applications, 2012

[42] GH Kimet al., *A moving mat: phototaxis in the filamentous green algae Spirogyra (Chlorophyta, Zygnemataceae)*, Journal of Phycology 41: 232-237, 2005

[43] KJ Kim, S Tadokoro (Eds), *Elecroactive Polymers for Robotic Applications, Artificial Muscles and Sensors*, Springer, 2007

[44] VD Kern et al., *Gravitropic moss cells default to spiral growth on the clinostat and in microgravity during spaceflight* , Planta, 221: 1, 149-157, 2005.

[45] JH Kyung, BG Ko, YH Ha, GJ Chung, *Design of a microgripper for micromanipulation of microcomponents using sma wires and flexible hinges*, Sens.Actuators A 141: 144-150, 2008

[46] M Kohl, *Shape memory microactuators*, New York, Springer, 2004.

[47] C-C Lan, J-H Wang, C-H Fan, *Optimal design of rotary manipulators using shape memory alloy wire actuated flexures*, Sensors and Actuators A 153: 258-266, 2009.

[48] C-C Lan, Y-N Yang, *A computational design method for a shape memory alloy wire actuated compliant finger*, ASME J. Mech. Des. 131 (2009) 021009

[49] C Laschi, B Mazzolai, M Cianchetti, L Margheri, M Follador and P Dario, *A Soft Robot Arm Inspired by the Octopus*, Adv. Robotics 26 709-726, 2011

[50] H Liss and EW Weiler, *Ion-Translocating atpases in tendrils of bryonia-dioica jacq*, Planta, 194(2), pp. 169-180, 1994.

[51] EV Mangan, DA Kingsley, RD Quinn and HJ Chiel, *Development of a Peristaltic Endoscope*, Proceedings of IEEE International Conference on Robotics and Automation, ICRA '02, 2002.

[52] RS Manning and KA Hoffman. *Stability of n-covered circles for elastic rods with constant planar intrinsic curvature*, J. Elast., 62:23-46, 2001.

[53] T. McMillen and A. Goriely. *Tendril Perversion in Intrinsically Curved Rods*, J. Nonlinear Sci. Vol. 12: pp. 241-281, 2002

[54] B Millet and PM Badot. *The revolving movement mechanism in Phaseolus; New approaches to old questions*. In: Greppin H, Degli Agosti R, Bonzon M, eds, Vistas on Biorhythmicity. University of Geneva 1996; 77-98.

[55] S Mugnai, E Azzarello, E Masi, C Pandolfi, S Mancuso, *Nutation in plants.* In: Mancuso S, Shabala S, editors. Rhythms in plants: phenomenology, mechanisms and adaptative significance. Springer; 2007. pp. 77–90.

[56] S Neukirch and A Goriely, *Twining plants: How stick should their supports be?*, Proc. 5th Plant Biomechanics Conference, Stockholm, Aug 28-Sept 1, 2006.

[57] TE Riehl and MJ Jaffe, *Physiological Studies on Pea Tendrils. XIV Effects of mechanical perturbation, light, and 2-deoxy-D-glucose on callose deposition and tendril coiling*, Plant Physiol., 75, 679-687, 1984.

[58] G Robinson and JBC Davies, *Continuum robots - a state of the art*, IEEE Int. Conf. Robot. Automation, 2849-2854, Detroit (USA), 1999

[59] J Von Sachs, *Lectures on the physiology of plants*, Oxford : The Clarendon Press , 1888.

[60] JK Salisbury, *Kinematic and Force Analysis of Articulated Hands.* Ph.D. Thesis (Stanford University, Stanford 1982)

[61] LC Trevisan Scorza and M Carnier Dornelas, *Plants on the move. Toward common mechanisms governing mechanically-induced plant movements*, Plant Signaling and Behavior 6:12, 1979-1986, 2011

[62] B Siciliano, O Khatib, *Handbook of Robotics*, Springer, 2008.

[63] M Sreekumar, T Nagarajan, M Singaperumal, *Experimental investigations of the large deflection capabilities of a compliant parallel mechanism actuated by shape memory alloy wires*, Smart Mater. Struct. 17 (2008) 065025.

[64] P Simons, *The action plant*, Blackwell, Oxford, UK, 1992.

[65] G Song, *Design and control of a nitinol wire actuated rotary servo*, Smart-Mater. Struct. 16 (2007) 1796-1801.

[66] M Stolarz, *Circumnutation as a visible plant action and reaction*, Plant Signaling & Behavior 4:5, 380-387; May 2009

[67] T Takahashi T, T Tsuboi, T Kishida, Y Kawanami, S Shimizu, M Iribe, T Fukushima and M Fujita, *Adaptive Grasping by Multi Fingered Hand with Tactile Sensor Based on Robust Force and Position Control*, IEEE International Conference on Robotics and Automation Pasadena,CA, USA, May 19-23, 2008

[68] J Tegin and J Wikander, *Tactile sensing in intelligent robotic manipulation - a review*, Industrial Robot: An International Journal, Volume 32, Number 1, 2005 , pp. 64-70(7)

[69] A Tronchet, Bull. Soc. Hist. Nat. Doubs, 65, 43-44, 1963.

[70] JG Turner, C Ellis, A Devoto, *The jasmonate signal pathway*, Plant Cell 14 Suppl: S153-S164, 2002

[71] KC Vaughn and AJ Bowling, *Biology and Physiology of Vines*, Horticultural Reviews, Volume 38, 2011.

[72] I Walker, D Dawson, T Flash, F Grasso, R Hanlon, B Hochner, W Kier, M Pagano, C Rahn and Q Zhang, *Continuum robot arms inspired by cephalopods*, Proc. SPIE, Vol. 5804 (2005) pp. 303-314

[73] I Walker, C Carreras, R McDonnell and G Grimes, *Extension versus bending for continuum robots*, Int. J. Adv. Robot. Syst. 3(2), 171-178, 2006

[74] Z Wang, G Hang, J Li, Y Wang, K Xiao, *A micro-robot fish with embedded SMA wire actuated flexible biomimetic fin*, Sens. Actuators A 144 (2008) 354-360.

[75] H Yousef, M Boukallel and K Althoefer, *Review-Tactile sensing for dexterous in-hand manipulation in robotics - A review*, Sensors and Actuators A 167 (2011) 171-187

[76] M Zrinyi, *Intelligent polymer gels controlled by magnetic fields*, Colloid & Polymer Science, 278(2):98-103, 2000.

[77] HJ Zhou and ZC Ou-Yang, *Spontaneous curvature-induced dynamical instability of Kirchhoff filaments: Application to DNA kink deformations*, J. Chem. Phys., 110:1247-1251, 1999.

[78] http://www.yawcam.com, accessed on December 2012

[79] Artificial Muscle incorporated, http://www.artificialmuscle.com , accessed December 2012

[80] Dinalloy inc., http://www.dynalloy.com , accessed December 2012

[81] EU Octopus FP7 project, *http://www.octopus-project.eu/* accessed on December 2012